

Early Paleozoic paleomagnetic poles from the western part of the North China Block and their implications

Baochun Huang^{a,b,*}, Zhenyu Yang^{b,c}, Yo-ichiro Otofujii^b, Rixiang Zhu^a

^a Institute of Geophysics, Chinese Academy of Sciences, Beijing 100101, China

^b Department of Earth and Planetary Sciences, Faculty of Science, Kobe University, Kobe 657-8501, Japan

^c Institute of Geomechanics, Chinese Academy of Geological Sciences, Beijing 100081, China

Received 29 July 1997; accepted 12 March 1999

Abstract

We collected 917 oriented drill-core samples (124 sites) from 22 units spanning the Early Cambrian to Middle Ordovician formations of the North China Block (NCB) to construct an apparent polar wander path (APWP) of the early Paleozoic for the NCB. Sampling areas are located in the Helanshan, Tongchuan–Hancheng and Yuncheng–Luliang regions along the margin of the Ordos Basin. Characteristic remanent magnetizations for five periods between the Cambrian and Ordovician are isolated from 281 samples by careful demagnetization. Directions cluster around northwesterly direction with upward shallow inclination and its antipode after tilt correction. Reliability of these five directions is ascertained through positive fold and reversal tests. The five Cambrian and Ordovician paleopoles plot in the present Atlantic Ocean, which is consistent with previously reported paleomagnetic poles. A newly constructed APWP between the Cambrian and Ordovician indicates that the NCB was located in the Southern Hemisphere around 15°S during Cambro–Ordovician time. Motion of the NCB between the Early and Middle Cambrian comprised: a counterclockwise rotation of $22.3^\circ \pm 7.0^\circ$ and a northward latitudinal displacement of $7.2^\circ \pm 6.8^\circ$. Combining the paleobiogeographic and paleoclimatic data with the paleomagnetic implies that the NCB was probably located in East Gondwana in the Early Cambrian, and may have separated from Gondwana in post-Early Cambrian time. The NCB is also inferred to have been located close to Siberia and North America during the Middle Ordovician. © 1999 Elsevier Science B.V. All rights reserved.

Keywords: North China Block (NCB); early Paleozoic; paleomagnetism; paleogeography; Apparent Polar Wander Path (APWP)

1. Introduction

China is a composite landmass formed by three major crustal blocks: the North China Block (NCB), the South China Block (SCB) and Tarim. Among the Chinese blocks, the NCB is of particular interest for

understanding the tectonic history of Asia and the global tectonics because of its large area and central position in east Asia (Zhao et al., 1992).

Much uncertainty about the Paleozoic paleogeography of the Chinese blocks still remains. Several paleontologic studies favor the hypothesis that the Chinese blocks were derived from Paleozoic Gondwana (e.g. Audley-Charles et al., 1988; Long and Burrett, 1989; Burrett et al., 1990). The Chinese blocks may

* Corresponding author. Tel.: +81-78-803-6478; Fax: +81-78-803-5757; E-mail: bchuang@mail.c-geos.ac.cn

have been an ancient equatorial archipelago lying between a northerly Siberia and a southerly Gondwana throughout the Paleozoic (Zhao et al., 1996). The early and middle Paleozoic paleomagnetic data from the SCB and Tarim suggest that they may have been very close to the Australian margin of Gondwana during that time (Zhao et al., 1996). Although almost all the early Paleozoic paleomagnetic data for the NCB suggest that the NCB was located near to the paleo-equator during that period, whether or not it had some affinities with the early Paleozoic Gondwana is less clear. The late Paleozoic paleomagnetic study, however, shows that the NCB was situated at a low to moderate latitude in the Northern Hemisphere, whereas Gondwana occupied a high latitude in the Southern Hemisphere during that time (Zhao et al., 1996). This implies that the NCB had already rifted from Gondwana by the late Paleozoic. The early and middle Paleozoic paleomagnetic study of the NCB, therefore, would provide constraints on the tectonic history of the block itself and afford a clue to the paleogeographic reconstruction between east Asia and its adjacent regions of the world.

Although many early Paleozoic paleomagnetic results are reported from the NCB, especially its eastern to middle part (Gao et al., 1983; Lin et al., 1985; Wu, 1988; Lin and Fuller, 1990; Zhao et al., 1992, 1993; Meng and Coe, 1992; Yang et al., 1996), most of them are questionable. (1) The number of samples is generally small (e.g. Gao et al., 1983; Ordovician poles reported by Lin et al., 1985 and Zhao et al., 1992). (2) Overprints are not completely erased (e.g. Wu, 1988) and some samples are only treated with blanked demagnetization techniques (Gao et al., 1983). (3) Uncertain ages are assigned to some paleomagnetic poles (e.g. Cambrian pole reported by Lin et al., 1985) or no field test is used to ascertain a pre-folding origin of the paleomagnetic directions (e.g. Yang et al., 1996). (4) Uncertain polarity is assigned to the paleomagnetic pole (e.g. Zhao et al., 1992, 1993). (5) Suspect local deformation or rotation is not precluded from the paleomagnetic poles for the Siluro–Devonian interval (Meng and Coe, 1992; Zhao et al., 1993). Therefore, more reliable Early Paleozoic paleomagnetic data are clearly desirable.

In this paper, we report of a paleomagnetic study on the Early Cambrian to Middle Ordovician strata

with definitively determined ages in the margin of the Ordos Basin of the NCB. On the basis of positive results of fold and reversal tests, characteristic directions that appeared after careful demagnetization to be primary magnetization of the early Paleozoic. Five paleomagnetic pole positions with ages ranging from the Early Cambrian to Middle Ordovician are established. Finally, we compare them with early Paleozoic results previously reported from the NCB, and discuss their paleogeographic implications together with paleobiogeographic and paleoclimatic data.

2. Geologic setting and paleomagnetic sampling

In the NCB, the Lower Paleozoic sequence is developed by the Cambrian and Lower Ordovician carbonate rocks of littoral to shallow-sea origin and the Middle Ordovician carbonate rocks of the open-sea facies (Yang et al., 1986). The margin of the Ordos Basin, to the west of the NCB, is fundamentally considered as the portion of the oldest heartland of this block. Although the western part of the NCB may have been strongly deformed during the Himalayan Stage, it appears to be more suitable for early Paleozoic paleomagnetic study than the eastern part of the NCB, which has been subjected to deformation by volcanism and folding since the Late Permian. For example, the Indosinian movement caused local overfolding and metamorphism in the Yanshan and northern Taihengshan areas (Yang et al., 1986). Three regions, comprising the margin of the Ordos Basin, i.e. Helanshan, Tongchuan-Hancheng, and Yuncheng-Luliang, were consequently chosen for paleomagnetic sampling (Fig. 1).

2.1. Helanshan area in Ningxia Hui autonomous region

This paleomagnetic sampling area is located in the middle to northern portion of Helan Mountain, the western margin of the Ordos Basin (locality H in Fig. 1). The oldest sedimentary unit of this region is the Lower Archeozoic Helanshan Group mainly distributed in the middle to northern portion of Helan Mountain. The Rb–Sr isochronal age of these highly metamorphosed rocks is about 2058

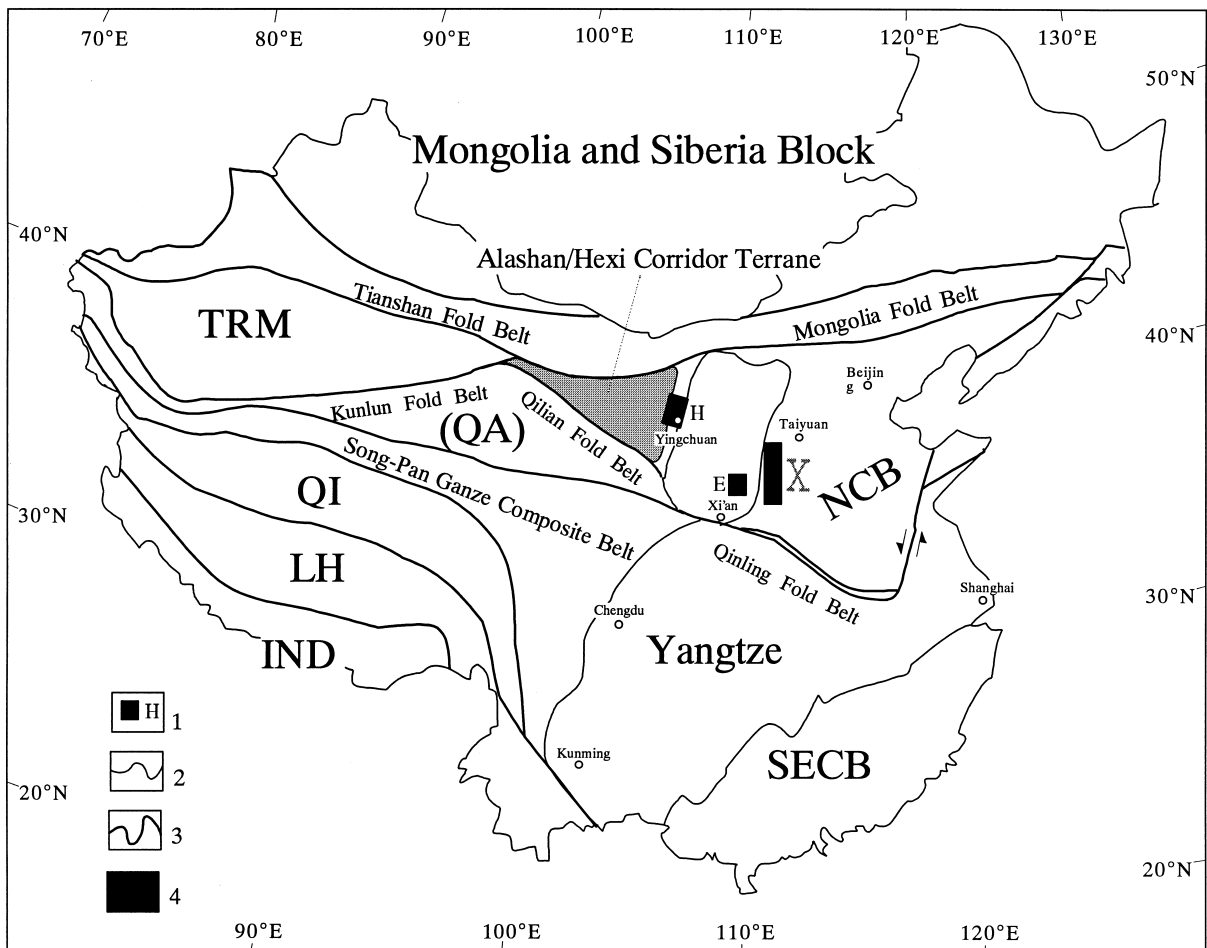


Fig. 1. Sketch map of the present location of continental blocks of China showing the tectonic framework, geotectonic units and paleomagnetic sampling regions modified after Cheng (1994). 1 = sampling region, H = Helanshan area, E = Tongchuan–Hancheng area, X = Yuncheng–Luliang area; 2 = fault and boundary of blocks; 3 = suture; 4 = Ordos Basin. NCB = North China block; Yangtze = Yangtze block; SECB = Southeast China block; TRM = Tarim block; QA = Qaidam block; QI = Qiangtang (North Tibet) block; LH = Lhasa (South Tibet) block; IND = India block.

Ma (NBGMR, 1990). The Cambro–Ordovician sediments reflect a continuous sedimentation with the basal unit in paraconformable contact with the underlying Sinian Zhenmuguan Formation, and belong to the stable type of platform deposition or marginal platform-type facies (NBGMR, 1990). Two major folding events occurred presumably in the Late Triassic and Early Cretaceous corresponding to the Indosinian movement and Yanshanian movement, respectively (NBGMR, 1990). A total of 324 oriented drill-core samples (45 sites) with ages ranging from Early Cambrian to Middle Ordovician were

collected from eight formations at four widely distributed localities (Table 1). The lithology of the Cambrian is dominated by limestone, dolomite and dolomitized limestone of a dark gray color. The Ordovician samples consist of gray to dark gray limestone and some purplish-red shale and sandstone (Table 1).

2.2. Tongchuan–Hancheng area in Shaanxi Province

The lower Paleozoic sediments of this area are mainly represented by limestone and dolomite rocks.

Table 1
Sampling details and corresponding rock magnetic experiments for the early Paleozoic paleomagnetic study in the west of the NCB

Site ID	Formation	Sampling location	S _{long.} (°E)/S _{lat.} (°N)	n/N	Lithology	Remarks
<i>Middle Ordovician</i>						
X33–X39	Fengfeng	Baiwapin, Zhongyang County, Shanxi	111.17/37.33	50/7	limestone	
E01–E07	Jinghe	Houdong, Tongchuan City, Shaanxi	109.04/36.05	45/7	limestone	
H24–H30	Pingliang	Yushugou, Yinchuan City, Ningxia	105.88/38.45	48/7	netted muddy limestone	A(2) B(3)
X26–X32	Upper Majiagou	Baiwapin, Zhongyang County, Shanxi	111.17/37.33	50/7	limestone	C(1)
<i>Lower Ordovician</i>						
E50–E55	Lower Majiagou	Shangyukou, Hancheng City, Shaanxi	110.57/35.63	41/5	dolomitic limestone	
E40–E46	Liangjiashan	Shangyukou, Hancheng City, Shaanxi	110.57/35.63	44/5	muddy limestone	
H10–H16	Tianjingshan	Dananchi, Yinchuan City, Ningxia	105.91/38.55	50/7	netted muddy limestone	A(4) B(4)
H17–H22	Miboshan	Dananchi, Yinchuan City, Ningxia	105.91/38.55	40/5	sandstone and limestone	A(2) B(2)
<i>Upper Cambrian</i>						
H61–H66	Changshan	Dadiangou, Inner Mongolia	106.85/38.72	31/4	limestone and dolomite	A(3) B(3)
E08–E14	Changshan	Baifangou, Hancheng City, Shaanxi	110.50/35.60	45/6	dolomite	
H54–H60	Gushan	Dadiangou, Inner Mongolia	106.85/38.72	45/7	limestone	A(3) B(3)
E16–E21	Gushan	Baifangou, Hancheng City, Shaanxi	110.50/35.60	37/5	limestone and dolomite	
X21–X23	Gushan	Baiwapin, Zhongyang County, Shanxi	111.20/37.30	23/3	limestone and shale	
<i>Middle Cambrian</i>						
X15–X20	Zhangxia	Baiwapin, Zhongyang County, Shanxi	111.20/37.30	36/5	limestone and dolomitic limestone	
E22–E27	Zhangxia	Baifangou, Hancheng City, Shaanxi	110.50/35.60	41/5	limestone and dolomitic limestone	
H31–H37	Zhangxia	Suyukou, Yinchuan City, Ningxia	105.90/38.75	49/7	limestone	A(2) B(3)
H40–H42	Xuzhuang	Suyukou, Yinchuan City, Ningxia	105.90/38.75	23/3	limestone	A(3) B(3)
X07–X14	Xuzhuang	Baiwapin, Zhongyang County, Shanxi	111.20/37.30	55/8	sandstone and limestone	A(2) C(2)
E28–E33	Xuzhuang	Baifangou, Hancheng City, Shaanxi	110.50/35.60	37/5	sandstone, shale, limestone and dolomitic limestone	
<i>Lower Cambrian</i>						
H45–H50	Wudaotang	Suyukou, Yinchuan City, Ningxia	105.90/38.75	38/5	dolomite and dolomitic limestone	A(3) B(3)
X01–X06	Xinji	Shuiyu Town, Ruicheng County, Shanxi	110.60/34.80	50/6	sandy shale and limestone	A(2) C(2)
E34–E39	Mantou	Baifangou, Hancheng City, Shaanxi	110.50/35.60	39/5	shale, mudstone, sandstone and dolomitic limestone	

Abbreviations: Site ID = site identification; S_{long.} (°E)/S_{lat.} (°N) = site longitude and latitude; n/N = number of samples and sites sampled. A(2) = rock magnetic experiment method (number of samples measured). A = acquisition and back-demagnetization of IRM; B = stepwise thermal demagnetization of composite IRMs following Lowrie (1990); C = low-temperature experiment.

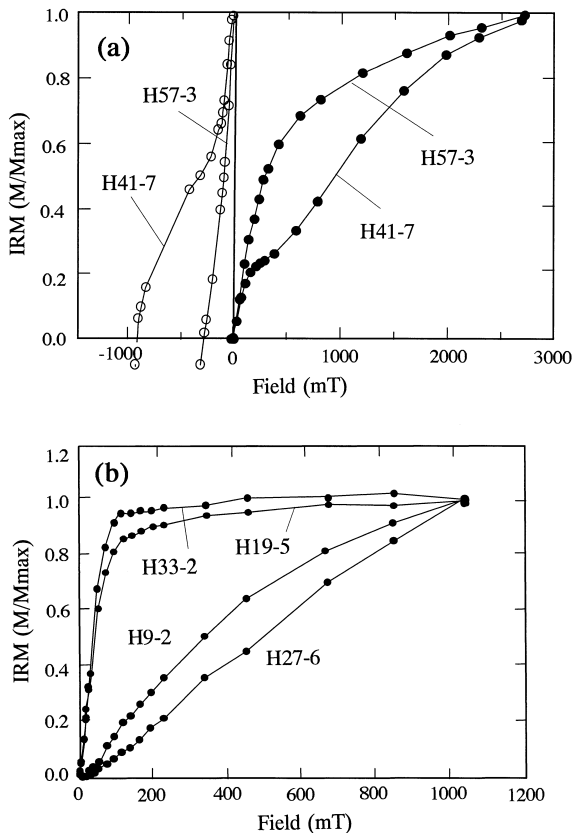


Fig. 2. Behavior of the acquisition and back-demagnetization of IRM. (a) Acquisition (solid circles) and back-demagnetization (open circles) curves of IRM. (b) Acquisition curve of IRM.

The ages of these sediments are well controlled with the abundance of many typical flora fossils, such as, *Redlichia chinensis* of the Mantou Formation, *Blackwelderia* of the Guoshan Formation, and *Polydesmia zuezshengensis* of the Majiagou Formation (SABGMR, 1989). Folding is thought to have occurred during the Early Jurassic to Early Cretaceous: two unconformities can be distinguished, the first one between Late Triassic and Early Jurassic sediments, and the second one between Middle Jurassic and Early Cretaceous sediments. Thirty-six sampling sites for the Cambrian and Lower Ordovician and seven sites for the Middle Ordovician are located at roadcuts and quarries close to Hancheng and Tongchuan cities, respectively (locality E in Fig. 1). Both the Cambrian and the Lower to Middle Ordovician rocks sampled consist of limestone and

dolomitized limestone with a gray and dark gray color. A total of 329 oriented drill-core samples were collected from eight formations (Table 1).

2.3. Yuncheng–Luliang area in Shanxi Province

The lower Paleozoic strata of this area were sampled in two separated localities (locality X in Fig. 1). The first locality is in Shuiyu village, about 100 km southwest of Yuncheng, the southernmost city of Shanxi Province. The Lower Cambrian Xinji Formation that unconformably overlies the Proterozoic conglomerate and conformably underlies the Mantou Formation, another Lower Cambrian formation, is considered to be correlated with the Suyukou Formation of Ningxia (SBGMR, 1989). Like most areas of the NCB, major folding is thought to be Late Triassic, associated with the Indosinian movement. A total of 50 oriented drill-core samples were sampled from 6 sites. The second locality is situated close to Zhongyang County, about 200 km southwest of Taiyuan City, the southeast margin of the Ordos Basin. Two hundred and fourteen (214) oriented drill-core samples were taken from 29 sites of 5 Lower Cambrian to Middle Ordovician formations along roadcuts. The sampled rocks consist of dark gray limestone and gray dolomitized limestone, except for purplish and red sandstone of the Xuzhuang Formation of Middle Cambrian age (Table 1). The Fengfeng Formation, the youngest in this sampling area, is unconformably overlain by the Middle Carboniferous Bengqi Formation.

A sampling site is generally composed of about seven independently oriented drill-core samples distributed stratigraphically over several meters. All the samples were oriented using a magnetic compass.

3. Rock magnetic study

Rock magnetic experiments were carried out to identify magnetic minerals in rocks of 55 pilot samples from 11 formations of the Helanshan and Yuncheng–Luliang areas (Table 1). This study shows that the main magnetic mineral is magnetite or hematite coexisting with pyrrhotite or maghemite. Measurements of remanent magnetization were carried out on a 2G Enterprises cryogenic magnetome-

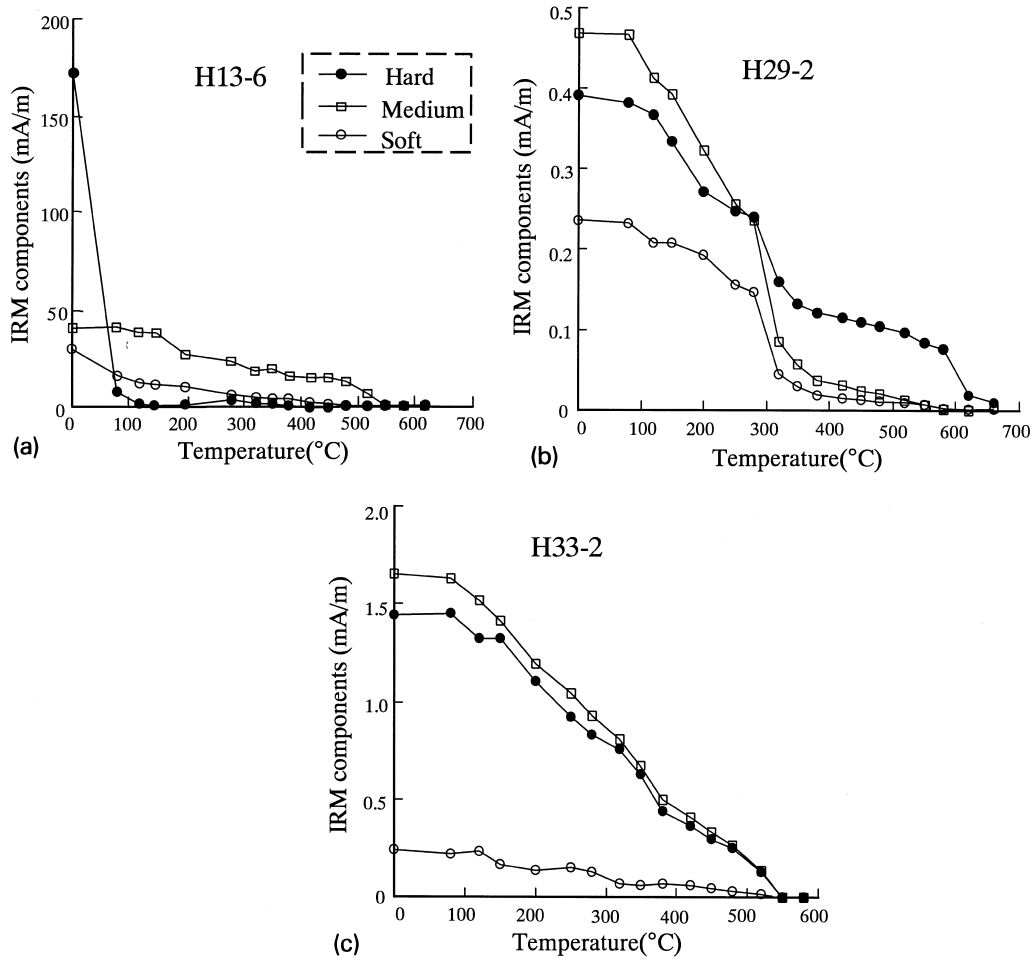


Fig. 3. Stepwise thermal demagnetization curves of the composite IRMs following Lowrie (1990).

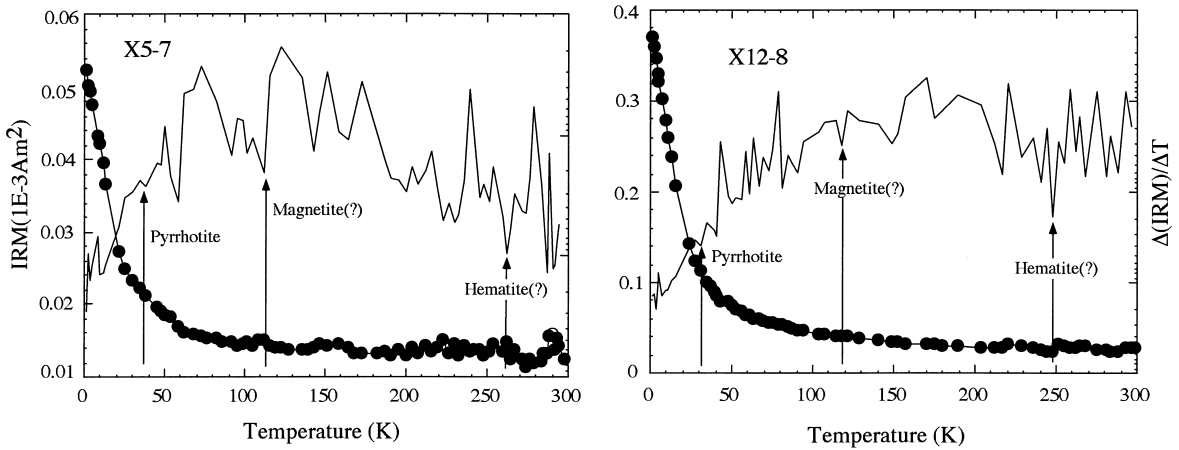


Fig. 4. Behavior of the IRM acquired at 1.5 K (5.0 T) warming to room temperature at 3–5 K intervals.

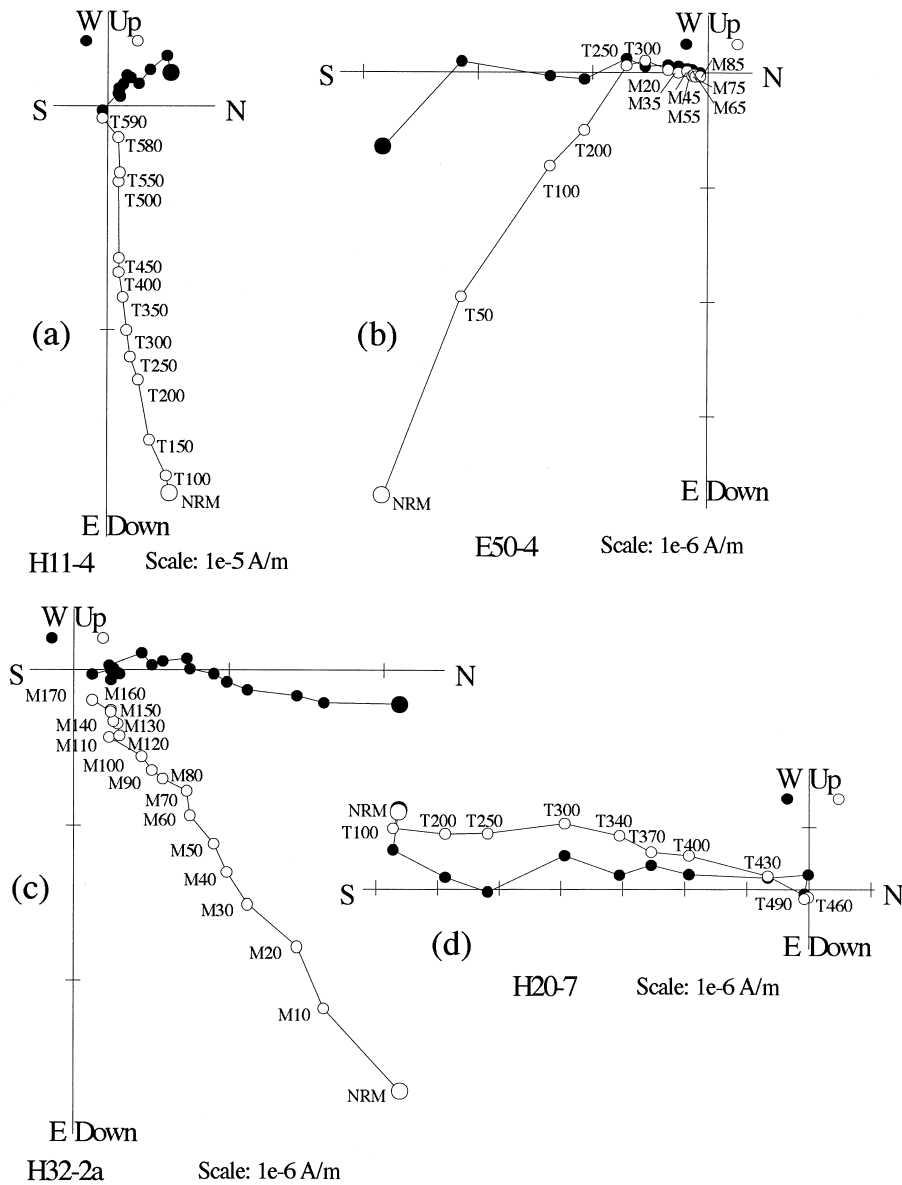


Fig. 5. Orthogonal vector plots of representative samples exhibiting only secondary magnetization. Directions are plotted in-situ, open and solid circles represent vector endpoints projected onto the vertical and horizontal planes, respectively. *T* and *M* imply thermal (°C) and AF (mT) demagnetization, respectively.

ter, with AF and thermal demagnetization performed on 2G and Schonstedt equipment, respectively.

Acquisition and back-demagnetization behavior of isothermal remanent magnetization (IRM) was observed for 26 samples. Most samples (17 samples) reveal a quasi-saturation behavior at about 0.2

T and a further gradual increase in IRM intensity up to 2.7 T (Fig. 2a). Combining remanent coercivity (H_{cr}) deduced from back-demagnetization, the main magnetic minerals in these samples are evidently composed of low-coercivity minerals (e.g. pyrrhotite, maghemite, magnetite) and medium- to

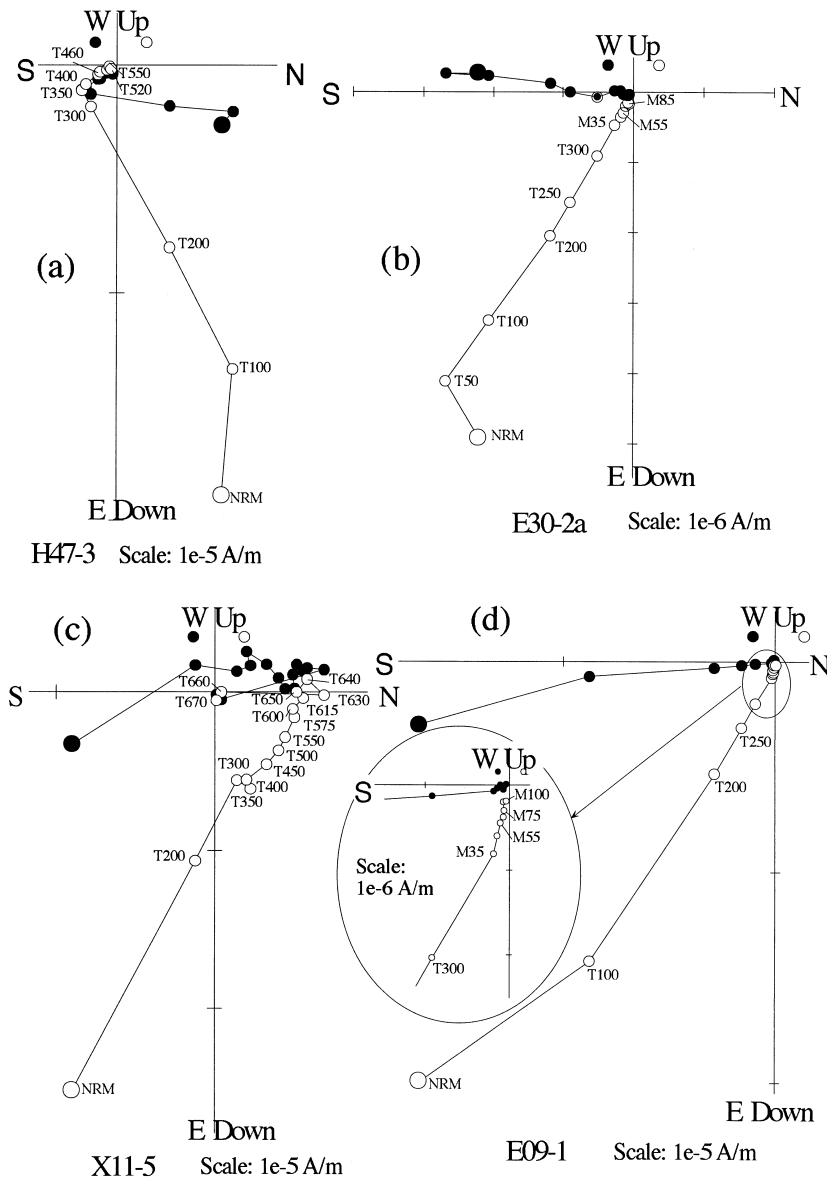


Fig. 6. Orthogonal vector plots of representative samples exhibiting characteristic component B for the Early Cambrian (a), the Middle Cambrian (b) and (c), the Late Cambrian (d).

high-coercivity ones (e.g. hematite). Some samples (6 Early Cambrian limestones) reach saturation at 0.1 T (Fig. 2b, H19-5 and H33-2) with remanent coercivity (H_{cr}) lower than 0.1 T (e.g. H34-1, Huang et al., 1995). This implies that magnetite or titanomagnetite is the predominant mineral. The remaining three samples (netted muddy limestones of the Middle Ordovician) show a linear increase in IRM inten-

sity up to 1.2 T (Fig. 2b, H27-6 and H9-2). The natural remanent magnetization (NRM) of these samples shows a weak intensity and low unblocking temperature ($<200^\circ\text{C}$). Goethite is possibly the main carrier.

The presence of magnetite and hematite is ascertained through thermal demagnetization of composite IRMs. A total of 24 samples were subjected to stepwise thermal demagnetization after applying

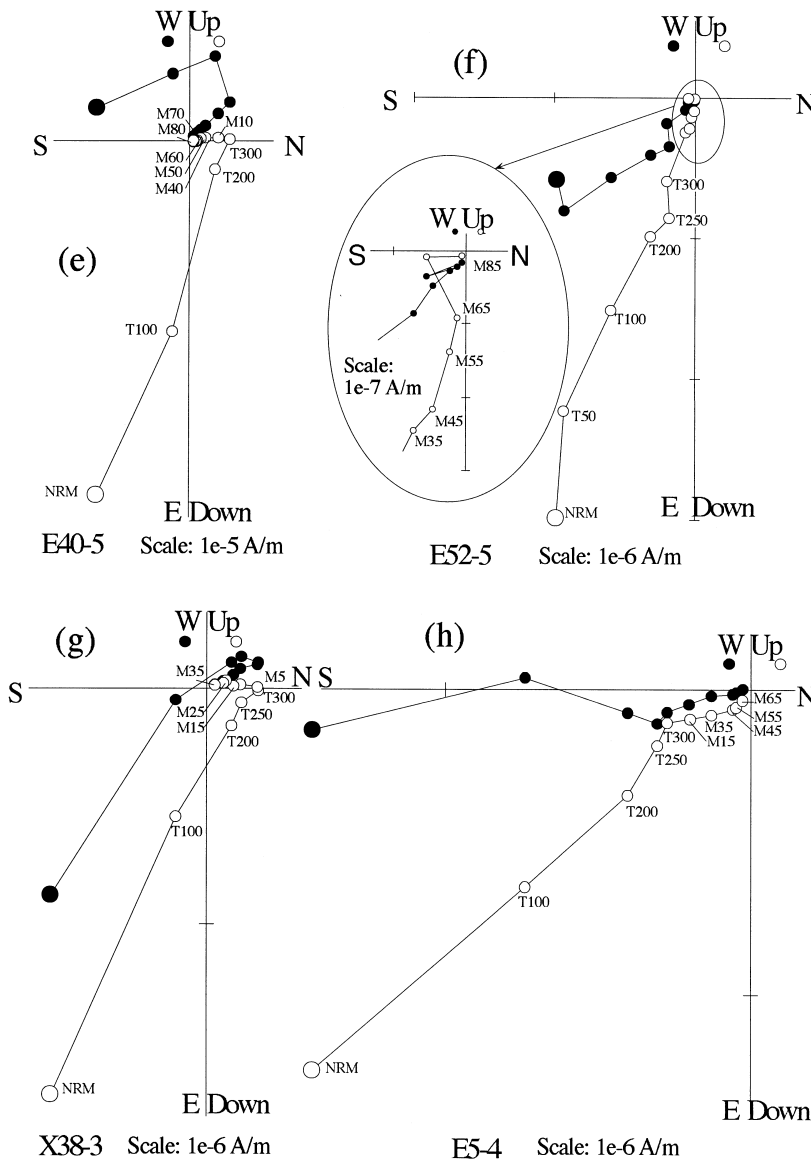


Fig. 6 (continued). The Early Ordovician (e) and (f), and the Middle Ordovician (g) and (h). The rest are as Fig. 5.

composite IRMs, following Lowrie (1990). DC magnetic fields of 2.7 T, 0.5 T and 0.05 T were applied to a sample Z-axis, Y-axis and X-axis separately using a 2G Pulse Magnetizer. Thermal demagnetization up to 680°C is performed.

Demagnetization of the composite IRMs suggests that the measured samples can be separated into three groups. (1) Unblocking temperatures at about 80°C were observed in the hard component, indicating the

presence of goethite. The soft and medium components are unblocked at 450–480°C and at 550°C, respectively. Magnetite with a broad range of titanium is the main magnetic carrier (Fig. 3a). (2) Unblocking temperatures at about 320°C were observed for all three components. The presence of pyrrhotite, greigite or maghemite is expected. The soft and medium components are unblocked around 580°C, indicating the presence of magnetite. Fur-

Table 2
Mean remanent directions and pole positions for component A of sampling units

Site ID	n/N	D_g (°)	I_g (°)	D_s (°)	I_s	κ_g	α_{95}	GP _{long.} /GP _{lat.} (°)	SP _{long.} /SP _{lat.} (°)
H24–H30	16/22	351.4	58.3	315.1	78.3	40.5	5.9	23.2/83.3	79.9/51.9
H31–H37	28/31	4.1	59.4	357.9	25.0	19.7	6.3	169.8/86.5	290.0/64.3
H40–H42	14/14	359.5	62.8	357.4	30.8	149.8	3.3	102.1/84.5	292.5/67.7
H45–H50	22/24	0.0	63.1	20.8	33.5	77.6	3.4	105.9/84.2	238.7/62.7
H54–H60	24/25	354.8	51.9	331.6	33.4	21.9	6.5	322.7/82.5	345.2/58.0
H61–H66	14/14	347.0	61.1	333.4	38.0	10.3	13.0	40.2/79.5	347.3/61.3
Fold test ($N = 6$)									
McElhinny's fold test (McElhinny, 1964): $K_g/K_s = 18.64 > F(10, 10) = 4.85$ indicates negative at the 99% confidence level									
H10–H16	29/34	276.4	80.5	222.6	74.2	47.1	4.0	82.2/38.2	85.7/15.0
H17–H22	12/23	140.0	−31.5	130.8	−35.3	7.3	17.2	175.6/−49.1	186.2/−43.6
X01–X06	34/38	170.7	−31.4	180.5	−26.4	7.8	9.4	137.9/−70.3	109.1/−69.1
X07–X14	21/40	140.8	−54.8	131.6	−31.7	6.4	13.7	209.7/−58.6	189.4/−43.1
X15–X20	11/20	143.9	−44.9	136.8	−25.7	5.6	21.3	192.2/−57.7	181.1/−44.8
X21–X23	6/18	124.5	−60.1	104.6	−39.7	10.3	21.9	224.1/−47.5	211.6/−24.7
X26–X32	6/42	132.3	−45.4	127.8	−25.9	13.5	18.9	200.8/−40.7	188.4/−38.1
X33–X39	18/48	313.7	60.0	301.0	36.1	18.4	8.3	41.6/54.3	19.7/36.3
E01–E07	4/32	164.8	−24.1	164.8	−24.1	4.4	49.5	143.2/−62.9	143.2/−62.9
E08–E14	19/37	300.9	67.5	125.1	62.6	12.9	9.7	59.0/45.6	146.7/3.9
E16–E21	22/29	140.3	−17.2	152.9	−37.7	17.4	7.6	173.7/−45.0	176.5/−62.2
E22–E27	7/30	130.0	9.4	132.9	−31.3	24.3	12.5	170.5/−28.2	189.0/−44.3
E28–E33	29/33	138.9	14.0	143.9	−38.4	8.5	9.8	161.1/−32.4	186.4/−55.6
E40–E46	26/27	199.7	59.3	227.0	35.8	22.3	6.1	95.3/−12.1	64.0/−18.9
E50–E55	15/32	153.5	40.4	155.4	−15.7	14.6	10.4	137.8/−26.2	155.6/−54.4
Fold Test ($N = 15$)									
McElhinny's fold test (McElhinny, 1964): $K_s/K_g = 0.63 < F(28, 28) = 1.88$ indicates inconclusive at the 95% confidence level									

Abbreviations: n/N = number of samples exhibiting component A/total samples demagnetized; D_g/I_g (D_s/I_s) = declination and inclination in situ (after tilt correction); GP_{long.}/GP_{lat.} (SP_{long.}/SP_{lat.}) = east longitude and north latitude of VGP in geographic (stratigraphic) coordinate. Coordinate system: subscripts 'g' and 's' represent geographic and stratigraphic coordinates, respectively. The rest same as Table 1.

thermore, the hard component is unblocked at about 660°C which indicates the presence of some hematite (Fig. 3b). (3) Thermal demagnetization of the soft, medium and hard components show unblocking temperatures of about 550°C (Fig. 3c). The main magnetic mineral is magnetite.

These experiments indicate that goethite is present only in netted muddy limestone of the Lower Ordovician Tianjingshan Formation. Pyrrhotite is possibly present in the lower Paleozoic rocks with the exception of the Lower Cambrian limestones. Magnetite is present in almost all early Paleozoic rocks, whereas hematite is included in the Late Cambrian dolomites and dolomitic limestones.

The presence of pyrrhotite is proved by its magnetic transition at about 32 K using a low-temperature superconducting magnetometer. A high DC magnetic

field (5.0 T) was imparted to the sample of the lower Paleozoic limestones, sandstones and sandy shales (Table 1) at about 1.5 K, followed by IRM measurements taken from 1.5 K to room temperature at 3–5 K intervals. After an abrupt drop of the IRM by super-paramagnetic minerals in the initial section of warming, a significant drop subsequently occurred at about 32 K (Fig. 4). This low-temperature phase transition is also detected as a singular point of finite difference [$\Delta(\text{IRM})/\Delta T$] curves for the sample (Fig. 4). Some pyrrhotite is obviously present (Dekkers et al., 1989; Rochette and Fillion, 1989; Rochette et al., 1990). The low-temperature transitions of magnetite and hematite for the sample of the Early and Middle Cambrian sandstones and sandy shales are not well detected owing to the instability of the finite difference curves when the temperature rises above

Table 3

Directions of the characteristic component B, pole positions and the associated statistical parameters for the early Paleozoic of the NCB — Middle Ordovician

Site ID	Strike/dip	N/R	D_g (°)	I_g (°)	D_s (°)	I_s (°)	κ_s	α_{95}	$P_{\text{long.}}(^{\circ})/P_{\text{lat.}}(^{\circ})$	$\delta p/\delta m$
E01	0/0	0/7	155.5	29.4	155.5	29.4	27.4	11.7	137.7/–33.2	7.1/12.9
E02	0/0	0/6	149.5	25.9	149.5	25.9	15.3	17.7	142.9/–32.6	10.3/19.1
E04	0/0	0/5	126.6	31.3	126.6	31.3	21.3	17.0	162.4/–16.9	10.7/19.0
E05	0/0	0/5	153.7	26.9	153.7	26.9	13.3	21.8	140.8/–33.9	12.9/23.7
E07	0/0	0/4	144.3	17.7	144.3	17.7	21.7	20.2	152.9/–33.8	10.9/20.9
H24–H25	80/28	0/4	137.5	51.0	147.9	26.0	14.7	24.8	142.4/–29.8	14.5/26.8
H26–H27	74/35	0/6	145.4	46.6	151.0	12.3	11.1	21.0	143.5/–37.8	10.9/21.4
X38	190/23	7/1	332.4	–8.4	337.6	–21.7	40.2	9.6	319.1/37.1	5.3/10.1
X39	190/23	10/1	310.9	0.4	312.9	–19.2	35.3	7.8	344.2/25.4	4.2/8.1
normal $N = 2$									332.4/31.9	
reversal $N = 7$									146.4/–31.4	$A_{95} = 7.6^{\circ}$
mean $N = 9$									327.7/31.5	$A_{95} = 7.0^{\circ}$

Fold test

(1) McElhinny's fold test (McElhinny, 1964): $K_s/K_g = 1.95 < F(16, 16) = 2.33$ indicates inconclusive at the 95% confidence level.

(2) McFadden and Jones's fold test (McFadden and Jones, 1981): $N = 9$, three localities: in geographic coordinate: $P = 3.81$; in stratigraphic coordinate: $P = 0.28$,

Reversal test

McFadden and McElhinny's reversal test (McFadden and McElhinny, 1990): $\gamma_c = 6.6^{\circ}$ indicates a B class reversal test result.

Abbreviations: Strike/dip = strike azimuth and dip of bed; N/R = number of samples exhibiting positive/negative polarity; $\delta p/\delta m$, the semi-axis of the confidence ellipse of VGP along or perpendicular to the great-circle path in stratigraphic coordinate. A_{95} = radius of circle of 95% confidence about the VGP in degrees in stratigraphic coordinates. The rest as Table 2.

Table 4

Directions of the characteristic component B, pole positions and the associated statistical parameters for the early Paleozoic of the NCB — Early Ordovician

Site ID	Strike/dip	N/R	D_g (°)	I_g (°)	D_s (°)	I_s (°)	κ_s	α_{95}	$P_{\text{long.}}(^{\circ})/P_{\text{lat.}}(^{\circ})$	$\delta p/\delta m$
E40	170/34	4/0	318.8	–4.8	326.5	–22.3	61.4	11.9	330.8/33.2	6.7/12.6
E41	170/34	2/0	317.6	–11.2	328.5	–27.0	–	–	327.2/31.9	–
E42	170/34	5/0	317.5	–11.6	328.6	–27.4	138.5	6.5	326.9/31.7	3.9/7.1
E45	170/34	5/0	312.6	3.3	316.0	–17.0	10.4	25.0	342.6/29.3	13.3/25.8
E50	50/50	0/6	188.2	53.5	167.0	12.3	106.7	6.5	129.5/–46.4	3.4/6.6
E51	48/49	0/4	199.1	53.5	171.2	18.1	207.6	5.6	122.8/–44.3	3.0/5.8
E52	48/49	0/6	134.1	78.7	137.1	29.7	81.8	7.5	156.5/–24.4	4.6/8.2
E53	75/57	0/3	161.4	63.8	163.4	6.8	39.4	19.9	135.7/–48.0	10.1/20.0
E55	75/57	0/6	149.6	74.1	160.7	17.5	13.6	18.8	136.6/–41.8	10.1/19.5
normal $N = 4$									331.9/31.7	$A_{95} = 7.4^{\circ}$
reversal $N = 5$									137.3/–41.6	$A_{95} = 13.2^{\circ}$
mean $N = 9$									324.3/37.4	$A_{95} = 8.5^{\circ}$

Fold test

McElhinny's fold test (McElhinny, 1964): $K_s/K_g = 6.34 > F(16, 16) = 3.37$ indicates positive at the 99% confidence level.

Reversal test

(1) McFadden and Jones's 'reversal test' (McFadden and Jones, 1981): $F = 3.590 < F(2, 14) = 3.74$ indicates positive 'reversal test' at 95% confidence limit.

(2) McFadden and McElhinny's reversal test (McFadden and McElhinny, 1990): $\gamma_c = 15.9^{\circ}$ indicates a C class reversal test result.

For abbreviations see Table 3.

Table 5

Directions of the characteristic component B, pole positions and the associated statistical parameters for the early Paleozoic of the NCB — Late Cambrian

Site ID	Strike/dip	N/R	D_g (°)	I_g (°)	D_s (°)	I_s (°)	κ_s	α_{95}	$P_{\text{long.}}(^{\circ})/P_{\text{lat.}}(^{\circ})$	$\delta p/\delta m$
E08	35/50	0/5	169.3	65.4	143.1	20.8	77.9	8.7	154.5/–32.0	4.8/9.2
E09	35/50	0/7	196.4	57.1	159.4	24.0	82.8	6.7	136.4/–38.0	3.8/7.1
E11	35/50	0/5	203.4	60.3	158.6	28.8	165.2	6.0	136.0/–35.1	3.6/6.6
E12	35/50	0/5	164.7	63.6	142.4	18.2	61.2	9.9	156.2/–32.8	5.3/10.3
E13	35/50	0/6	188.1	53.4	159.0	18.0	79.0	7.6	138.4/–41.0	4.1/7.9
E14	35/50	0/9	176.1	61.0	148.5	19.2	77.4	5.9	149.8/–35.7	3.2/6.1
E18	10/31	0/5	169.7	50.3	145.6	33.0	18.0	18.5	147.7/–27.3	11.9/21.0
E19	10/31	0/5	165.0	49.1	143.5	30.4	12.8	22.2	150.6/–27.6	13.7/24.7
E20	10/31	0/5	146.4	49.8	131.1	25.1	28.8	14.5	163.3/–22.8	8.4/15.6
E21	10/31	0/4	164.8	52.1	141.4	32.8	14.7	24.8	151.5/–25.2	15.9/28.1
H57–H60	200/30	10/0	316.3	10.9	316.9	–16.1	12.0	14.5	337.0/28.0	7.7/14.9
normal $N = 1$									337.0/28.0	
reversal $N = 10$									148.8/–32.0	$A_{95} = 5.8^{\circ}$
mean $N = 11$									329.6/31.7	$A_{95} = 5.4^{\circ}$

Fold test

(1) McElhinny's fold test (McElhinny, 1964): $K_s/K_g = 4.80 > F(20, 20) = 2.94$ indicates positive at the 99% confidence level.

(2) McFadden and Jones's fold test (McFadden and Jones, 1981): $N = 11$, two localities: in geographic coordinate: $P = 10.05$; in stratigraphic coordinate: $P = 0.66$, $F(2, 18) = 3.55$ at the 95% confidence level indicative of positive regional 'fold test'.

For abbreviations see Table 3.

about 50 K. Nevertheless, the Verwey transition and the isotropic point in magnetite are sensitive to the effects of non-stoichiometry, cation substitution, and grain size (Moskowitz et al., 1998). The lack of low-temperature transition at 120 K would suggest that the magnetite is probably present in single domains (Halgedahl and Jarrard, 1995).

4. Paleomagnetic study

Six hundred and fifty-two (652) samples were paleomagnetically measured using three demagnetization techniques in the laboratory: AF, thermal, and a hybrid AF–thermal demagnetization. In most cases, AF treatment did not succeed in demagnetizing the NRM to a very weak remanence. Stepwise thermal demagnetization was chosen for the major part of the samples with temperature intervals ranging from up to 100°C at the lower temperature to 10°C at the higher temperature. Usually, after about 60% of remanent magnetization was removed at 250°C, magnetization directions became unstable probably due to weak magnetization or ther-

mochemical alteration. In this case, samples were subjected to a hybrid demagnetization technique, in which thermal demagnetization up to 250°C or 300°C is followed by AF demagnetization up to about 100 mT. All the demagnetization results were plotted as orthogonal diagrams (Zijderveld, 1967) and stereographic projections. The magnetic components were separated using principal component analysis (Kirschvink, 1980).

4.1. Magnetic component analysis

Most samples of the lower Paleozoic display a simple demagnetization behavior during AF, thermal or hybrid demagnetization (Figs. 5 and 6). Generally, after removing the present geomagnetic field overprints or viscous remanent magnetizations at the beginning of demagnetization, a higher temperature or coercivity component is isolated from most of the samples.

One group of directions (labeled component A) clusters mostly in the northwest with downward shallow to moderate inclination and its antipode after tilt correction. This component is unblocked at

Table 6

Directions of the characteristic component B, pole positions and the associated statistical parameters for the early Paleozoic of the NCB — Middle Cambrian

Site ID	Strike/dip	N/R	D_g (°)	I_g (°)	D_s (°)	I_s (°)	κ_s	α_{95}	$P_{long.}$ (°)/ $P_{lat.}$ (°)	$\delta p/\delta m$
E22	22/43	0/6	172.5	50.9	147.9	20.9	60.3	8.7	149.8/−34.6	4.8 9.1
E23	22/43	0/6	164.5	51.5	143.4	18.3	59.5	8.8	155.3/−33.3	4.7 9.1
E24	22/43	0/4	173.3	52.5	147.3	22.4	48.0	13.4	149.9/−33.5	7.5 14.2
E25	22/43	0/4	155.5	45.3	141.5	10.0	143.6	5.0	160.3/−35.6	2.6 5.1
E26	22/43	0/5	150.2	59.6	131.6	21.2	49.5	11.0	164.5/−24.8	6.1 11.6
E27	22/43	0/5	192.8	59.1	150.1	34.8	78.0	8.7	142.8/−28.3	5.8 10.0
E28	30/57	0/6	173.8	53.9	148.7	8.6	36.3	11.3	153.4/−40.5	5.7 11.4
E30	30/57	0/7	176.4	62.8	143.4	15.8	91.1	6.4	156.2/−34.4	3.4 6.5
E31	30/57	0/5	178.6	60.6	145.8	15.0	85.9	8.3	154.1/−36.1	4.4 8.5
E32	30/57	1/4	189.4	66.6	143.8	22.4	19.6	17.7	153.3/−31.6	9.9 18.8
E33	30/57	0/6	181.8	68.0	140.7	20.9	23.6	14.1	156.8/−30.6	7.8 14.8
X08	197/25	2/3	154.4	23.1	166.5	38.2	47.5	11.2	125.7/−29.9	7.9 13.3
X10	197/25	1/3	160.5	−7.6	160.5	7.4	21.8	20.1	139.4/−45.1	10.2 20.2
X11	197/25	4/0	350.3	3.9	351.0	−7.4	52.7	12.8	304.7/48.1	6.5 12.9
X18	200/20	0/6	157.8	2.3	160.2	15.5	16.2	17.2	137.7/−41.2	9.1 17.7
H31–H33	260/35	4/1	346.0	26.1	346.4	−8.8	12.7	22.3	305.3/45.0	11.4 22.5
H35–H33	260/35	3/0	341.6	27.5	342.5	−7.2	27.8	23.8	310.9/44.7	12.1 24.0
normal $N = 3$									307.0/46.0	$A_{95} = 4.6^\circ$
reversal $N = 14$									150.2/−37.0	$A_{95} = 5.0^\circ$
mean $N = 17$									326.7/37.0	$A_{95} = 5.5^\circ$

Fold test

(1) McElhinny's fold test (McElhinny, 1964): $K_s/K_g = 3.62 > F(32, 32) = 2.32$ indicates positive at the 99% confidence level.

(2) McFadden's fold test (McFadden, 1990): $N = 17$: in geographic coordinate: $\xi_1 = 8.114$; in stratigraphic coordinate: $\xi_1 = 1.048$, critical value of the test statistic $\xi = 6.721$ at the 99% confidence level indicative of positive fold test.

For abbreviations see Table 3.

Table 7

Directions of the characteristic component B, pole positions and the associated statistical parameters for the early Paleozoic of the NCB — Early Cambrian

Site ID	Strike/dip	N/R	D_g (°)	I_g (°)	D_s (°)	I_s (°)	κ_s	α_{95}	$P_{long.}$ (°)/ $P_{lat.}$ (°)	$\delta p/\delta m$
H45	315/45	0/3	150.6	21.6	129.7	26.0	124.6	11.1	158.4/−19.6	6.5/12.0
H46–H47	315/45	0/5	147.8	29.4	121.1	28.9	497.0	3.4	163.7/−12.8	2.1/3.8
H48	315/25	0/4	149.2	31.4	132.9	34.0	67.7	11.3	152.6/−17.6	7.4/12.9
H49	315/25	0/4	152.9	25.8	139.5	30.8	335.7	5.0	148.4/−22.9	3.1/5.6
H50	315/25	0/4	130.7	35.5	114.7	30.0	17.8	22.4	167.8/−8.0	13.8/24.9
X2	340/27	0/2	141.7	29.9	130.3	18.7	–	–	166.9/−25.4	–
X5	355/12	0/5	131.9	28.2	128.1	19.7	14.8	20.6	168.2/−23.5	11.3/21.5
X6	355/12	0/5	128.2	35.9	123.4	26.8	170.2	5.9	168.6/−17.4	3.5/6.4
mean $N = 8$									341.9/18.5	$A_{95} = 6.5^\circ$

Fold test

(1) McElhinny's fold test (McElhinny, 1964): $K_s/K_g = 1.40 < F(14, 14) = 2.48$ indicates inconclusive at the 95% confidence level.

(2) McFadden and Jones's fold test (McFadden and Jones, 1981): $N = 8$, two locations in geographic coordinate: $P = 5.99$; in stratigraphic coordinate: $P = 3.19$, $F(2, 12) = 3.89$ at the 95% confidence level indicative of positive regional 'fold test'.

For abbreviations see Table 3.

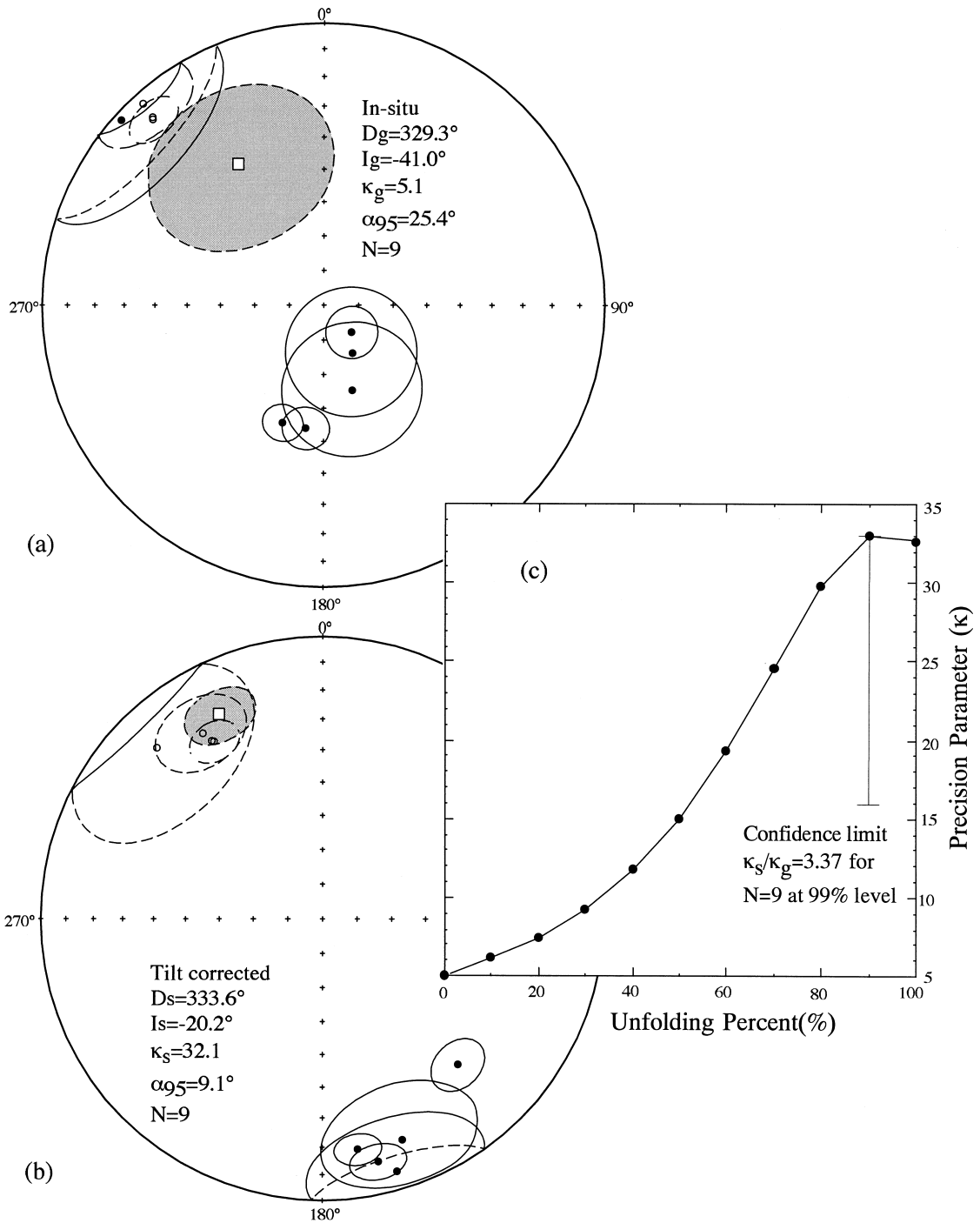


Fig. 7. Equal-area projection of site-mean directions of characteristic component B from the Lower Ordovician of the Hancheng area (a) before and (b) after tilt correction; solid/open symbols represent directions plotted onto the lower/upper hemisphere with 95% confidence limits. Squares represent mean directions. (c) Increment unfolding analysis.

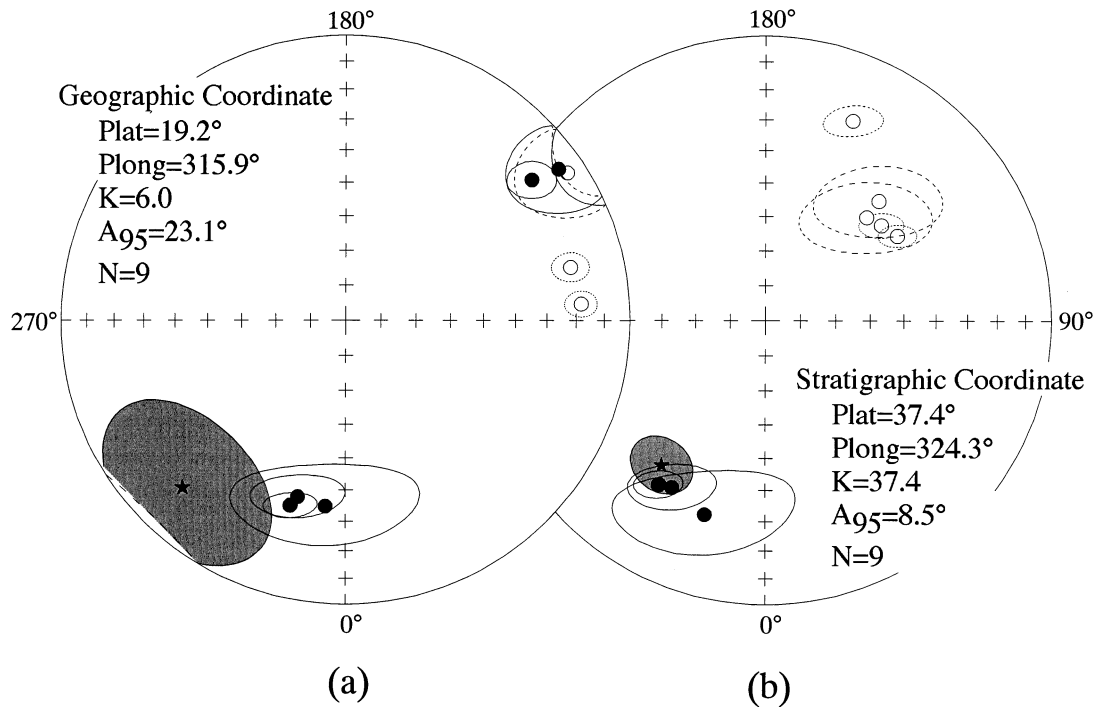


Fig. 8. Equal-area projection of the Middle Ordovician site-mean VGPs that joined the final statistical calculation under (a) geographic and (b) stratigraphic coordinates. Solid/open symbols represent VGPs plotted onto the lower/upper hemisphere with 95% confidence limits. Stars indicate mean VGP positions; circles, triangles, and squares represent VGPs from Tongchuan–Hancheng, Helanshan, and Yuncheng–Luliang sampling areas, respectively.

350–550°C in carbonate rocks and at 630–650°C in sandstones and shales (Fig. 5). AF demagnetization also shows that this component has a relatively high coercivity (Fig. 5c). Demagnetization behavior, combined with rock magnetic experiments, demonstrate that component A is carried by either pyrrhotite and maghemite in carbonates or hematite in sandstones and shales.

Another group of directions (labeled component B) tends toward the southeast with downward shallow inclination and its antipodal after tilt correction. This component is generally unblocked at about 500–550°C (Fig. 6a). In the case of the purplish-red sandstones and shales, component B is unblocked at 650–670°C (Fig. 6c). Component B can usually be demagnetized when the AC field increases to 40–80 mT in the course of the hybrid demagnetization of some carbonate rocks (Fig. 6b, d–h). The magnetic carrier of this component is principally either magnetite in the carbonate rocks or hematite in the purplish red sandstones and shales. The mean direc-

tions of components of A are listed in Table 2 and those of B are listed in Tables 3–7.

Some carbonate rocks (about 10 to 15%) reveal either a weak NRM intensity before treatment or an abrupt decrease in intensity after demagnetization at 10–20 mT or 100–200°C. Noisy behavior arises during further demagnetization, so that no characteristic direction is isolated.

4.2. Field test for stability of magnetization

The fold test is used to relate components of A and B to the regional folding.

4.2.1. Component A

With the exception of the Lower Ordovician formations, the A component isolated from the Helanshan area has a significant negative fold test at the 99% confidence level ($K_g/K_s = 18.64$, Table 2) according to McElhinny's test (McElhinny, 1964). The corresponding in-situ mean pole is at 49.7°E, 86.5°N

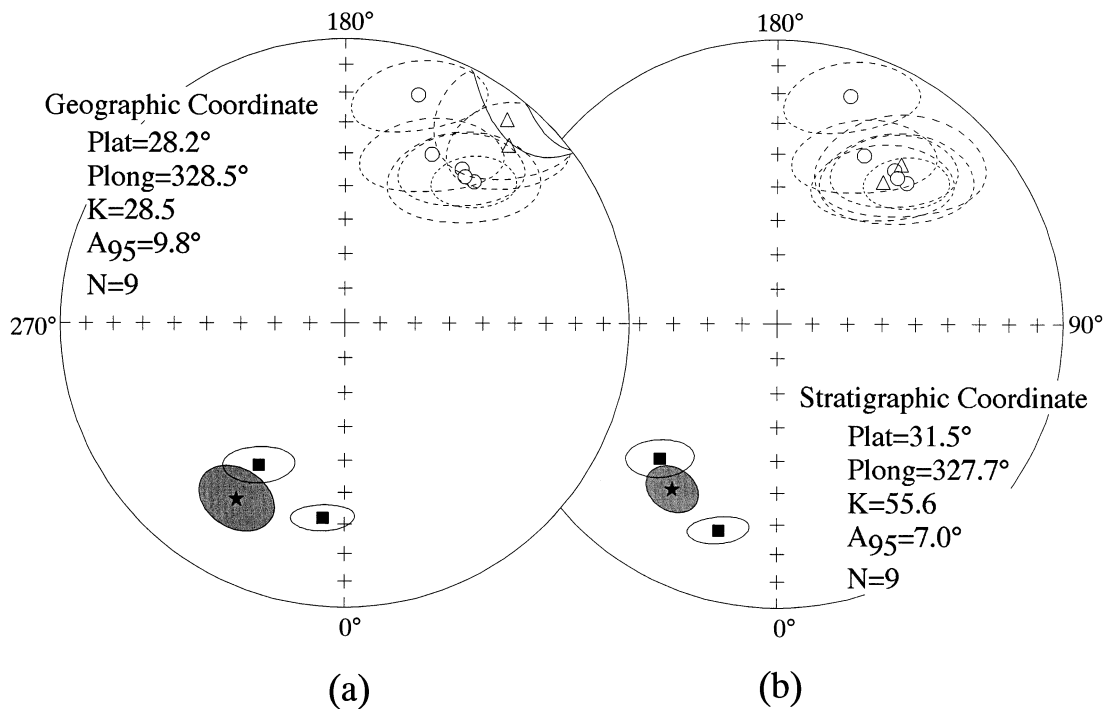


Fig. 9. Equal-area projection of the Early Ordovician site-mean VGPs that joined the final statistical calculation under (a) geographic and (b) stratigraphic coordinates. Symbols as Fig. 8.

with $K = 156.6$, $A_{95} = 5.4^\circ$, and is not significantly different from the Tertiary pole for the NCB (Zhao et al., 1994) at the 95% confidence limit according to the method of McFadden and McElhinny (1990). This indicates that the A component from the Cambrian and Middle Ordovician formations of the Helanshan area is of a post-Early Cretaceous folding origin and was probably acquired during the Tertiary.

The A component from the Lower Ordovician formations of the Helanshan area and the other two sampling areas, Tongchuan–Hancheng and Yuncheng–Luliang, yields an inconclusive fold test at the 95% confidence level ($K_g/K_s = 1.59$, Table 2) using the method of McElhinny (1964). However, the corresponding in-situ mean pole of 2.0°E , 53.7°N with $A_{95} = 17.2^\circ$ and the pole from the tilt-corrected direction (9.7°E , 56.9°N with $A_{95} = 23.1^\circ$) are located close to the Triassic pole for the NCB (Zhao et al., 1994) at the 95% confidence level according to the method of McFadden and McElhinny (1990). This indicates that the A component from these formations was probably acquired during the early Mesozoic.

4.2.2. Component B

The Early Ordovician samples were collected from two sections of the Tongchuan–Hancheng area with distinct dip directions, which allows the fold test to be applied. Clustering of the component B directions for these samples is strikingly improved after unfolding (Fig. 7). Component B yields a positive fold test at the 99% confidence level ($K_s/K_g = 6.34$, see Tables 3 and 4) (McElhinny, 1964), indicating a pre-folding origin. The consistency analysis (McFadden and Jones, 1981) of the normal and reversed directions shows that they share the same component, which is indicative of a positive reversal test for component B ($\gamma_c = 15.9^\circ$, C class reversal test result according to the method of McFadden and McElhinny (1990), Tables 3 and 4). Consequently, component B of the Early Ordovician from the Tongchuan–Hancheng area passes both positive fold and reversal tests, and is therefore presumed to be representative of the paleogeomagnetic field record close to the formation of the rocks.

The regional consistency test is given by the com-

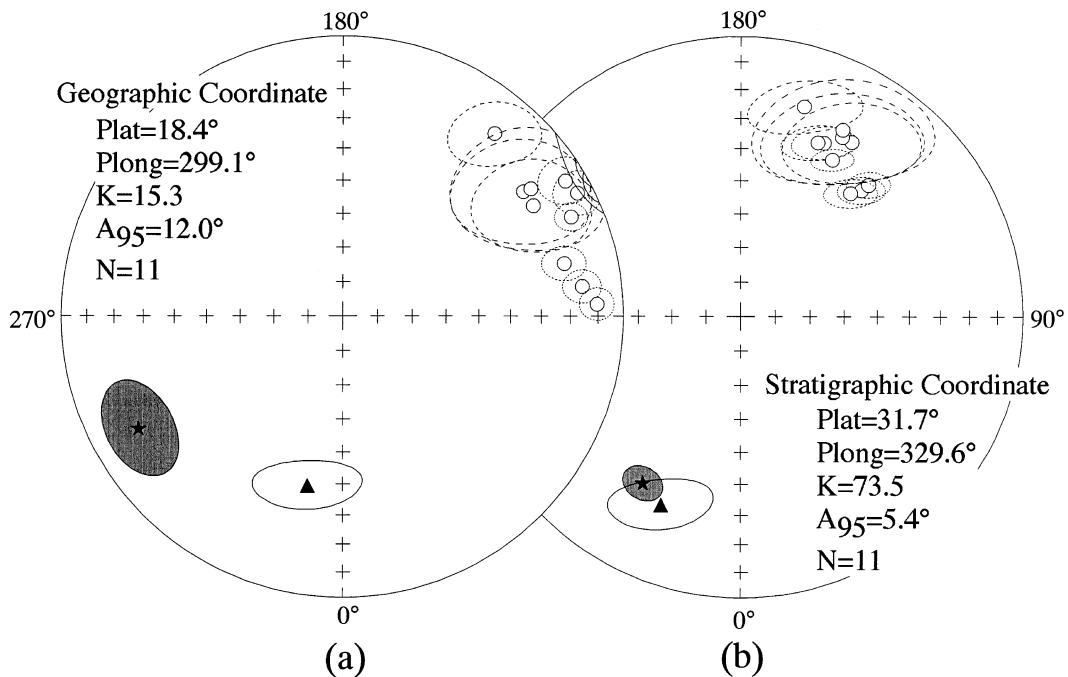


Fig. 10. Equal-area projection of the Late Cambrian site-mean VGPs that joined the final statistical calculation under (a) geographic and (b) stratigraphic coordinates. Symbols as Fig. 8.

parison of paleomagnetic results from the different localities. We first calculate the VGP from an individual site, then compare the statistical precision parameter changes before and after tilt corrections. McElhinny's statistic method (McElhinny, 1964) is used to judge the paleopole consistency for the Middle and Late Cambrian. The precision parameters of site-mean poles calculated from individual VGPs are significantly increased in stratigraphic coordinate (Tables 5 and 6; Figs. 8–11), indicative of positive regional 'fold tests'. The statistic precision parameter change is insignificant for the Early Cambrian and Middle Ordovician results (Figs. 8 and 12); however, the 'fold test' is positive using the *F*-test of McFadden and Jones (1981). The Middle Cambrian results obtained from the three localities Helanshan, Tongchuan–Hancheng, and Yuncheng–Luliang are statistically identical using McFadden's new fold test (McFadden, 1990) (see Table 6).

Thus we conclude that component B is of pre-folding origin on the basis of the positive fold test from the Early Ordovician formations of the Tongchuan–Hancheng area, and on the basis of a regional

paleopole consistency for the Cambrian and Middle Ordovician. On the other hand, it possesses both normal and reversed polarity for the Middle and Late Cambrian and Early and Middle Ordovician, which passed the reversal test. We believe that component B is primary with little or no contamination by unrecovered secondary magnetization, because it is carried by both magnetite and hematite, and is observed in rocks of different lithologies from widely distributed localities.

The site-mean directions of the characteristic component B, paleomagnetic results and associated statistical parameters are summarized in Tables 3–7.

5. Discussion

5.1. Assessment of magnetic polarity

Identification of the polarity of the paleomagnetic directions in the early Paleozoic is controversial in paleomagnetic studies of the NCB. Because of the paucity of reliable paleomagnetic data for the early

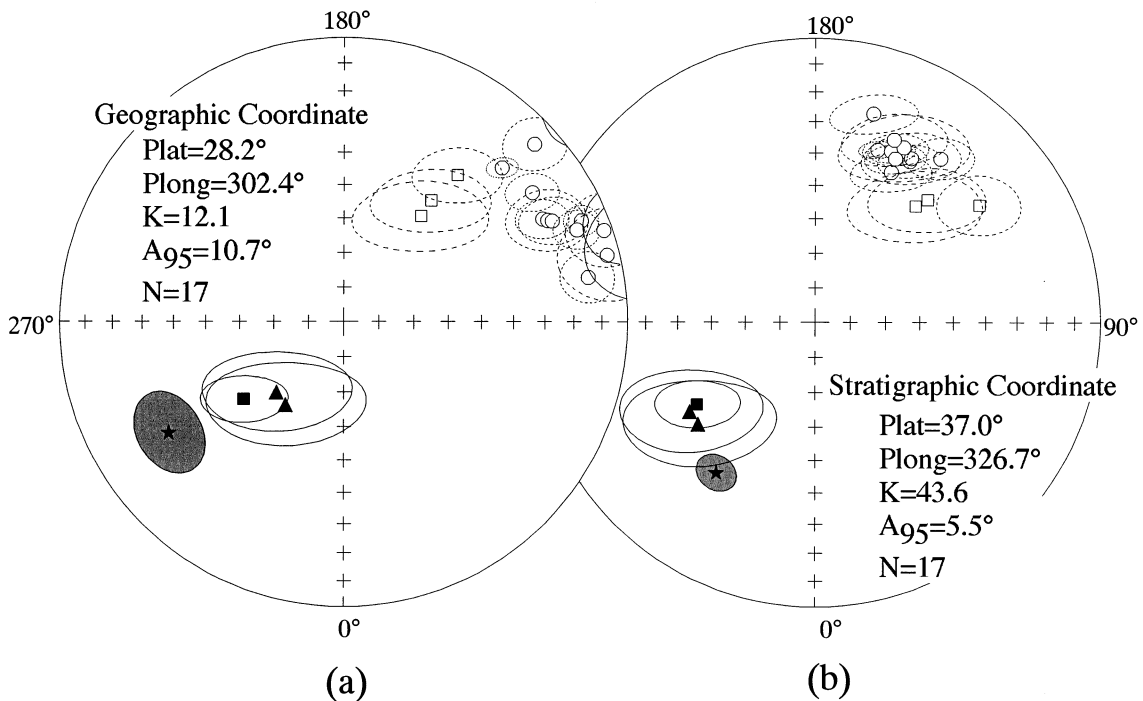


Fig. 11. Equal-area projection of the Middle Cambrian site-mean VGP that joined the final statistical calculation under (a) geographic and (b) stratigraphic coordinates. Symbols as Fig. 8.

Paleozoic and because data on the great sedimentary hiatus are lacking during the Late Ordovician to Early Carboniferous in the NCB, it is difficult to extrapolate younger paleomagnetic data backwards in time to determine the polarity of the early Paleozoic paleomagnetic direction (Zhao et al., 1992).

Except the results from the Fengfeng Formation (late-Middle Ordovician, Llandeilo stage; Yang et al., 1986) and the Liangjiashan Formation (early-Early Ordovician, early Arenig stage), we isolate a single polarity characteristic direction from the Middle Ordovician Jinghe (Llanvirn stage) and Pingliang (early Llandeilo stage; Yang et al., 1986) formations, and the late-Early Ordovician Lower Majiagou Formation (late Arenig stage) (see Tables 3–7). Yang et al. (1996) discovered only one polarity direction from the Middle Ordovician rocks (Upper Majiagou Formation, Llanvirn stage) from the Henan Province of North China. These results imply that one polarity probably prevailed in the period of the late-Early to Middle Ordovician (late Arenig and Llanvirn stages). From a large number of compilations of Paleozoic

paleomagnetic data, Johnson et al. (1995) and Algeo (1996) suggest that the Early and Middle Ordovician was probably a long interval of reversed polarity with a very low reversal rate. This estimate has recently been confirmed by the magnetostratigraphic studies in Siberia. A 25–30 m.y. period reversed superchron (or a very low magnetic reversal frequency) was suggested during the Arenig and Llanvirn stages (see details in Gallet and Pavlov, 1996; Pavlov and Gallet, 1998). This indicates that our results from the Jinghe, Pingliang and Lower Majiagou formations were induced during an interval of reversed polarity. The Middle Ordovician paleo-north pole therefore lies in the present Atlantic Ocean. The assessment of the polarity for the other early Paleozoic paleomagnetic directions is in accordance with this paleo-north pole position.

5.2. *Paleopoles comparison*

The reliability of our data is further ascertained by the close correspondence between the Cambrian

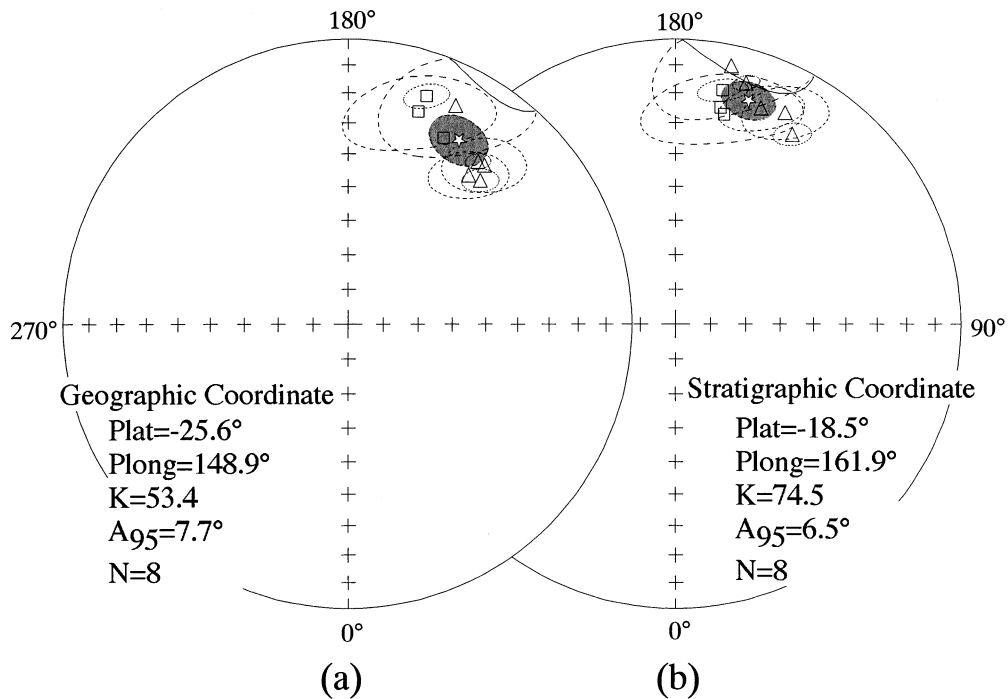


Fig. 12. Equal-area projection of the Early Cambrian site-mean VGPs that joined the final statistical calculation under (a) geographic and (b) stratigraphic coordinates. Symbols as Fig. 8.

and Ordovician paleopoles of this study and previously reported ones. Three Cambrian poles of this study form a cluster with that of Zhao et al. (1992) and Gao et al. (1983). The Cambrian pole of Zhao et al. (1992) (155.2°E , 21.2°S , $A_{95} = 12.4^{\circ}$) is reported from the latest-Precambrian–Early Cambrian to Late Cambrian shales, limestones and dolomites from three widely distributed localities in Hebei and Shandong Provinces and passes the fold, baked contact and reversal tests. This Cambrian pole and that of Gao et al. (1983) (334.5°E , 26.8°N , $A_{95} = 8.9^{\circ}$, after reanalysis of Zhao et al., 1992) lie between two poles of the Early and Middle Cambrian of our study, indicating no significant difference in position among them (Fig. 13).

Two other Cambrian poles are reported from Early Cambrian (Mantou Formation) red marl samples of the Shaanxi Province (Wu, 1988), and from three Cambrian red oolitic dolomite and limestone formations of the Shandong and Liaoning Provinces (Lin et al., 1985; Lin and Fuller, 1990). The pole of the former study (217.2°E , 15.3°N , $A_{95} = 17.5^{\circ}$) seems to be obtained from paleomagnetic compo-

nents in which secondary magnetization is not completely erased, because we failed in isolating the characteristic direction from the same formation (5 sites) in the same locality through careful demagnetization. The latter pole (298.6°E , 15.0°N , $A_{95} = 9.9^{\circ}$) might be reliable; however, the uncertain assignment in age, limited number of samples and the rough agreement with the Early Cambrian pole of North Korea (Gurarii et al., 1966) are pointed out by Zhao et al. (1992). We recognize these two Cambrian poles as unreliable.

Two Ordovician poles from our study lie in the proximity of the Ordovician poles of Zhao et al. (1992), Yang et al. (1996) and Lin et al. (1985). The Ordovician pole position (130.9°E , 28.8°S , $A_{95} = 12.3^{\circ}$) of Zhao et al. (1992) is similar to our Lower and Middle Ordovician poles within the 95% confidence limit (Fig. 13). Another Middle Ordovician pole (310.4°E , 27.9°N , $A_{95} = 9.2^{\circ}$) is reported from the Upper Majiagou Formation of Henan Province (Yang et al., 1996). Although no field test is used to ascertain a pre-folding origin for the characteristic direction of this pole, it lies at

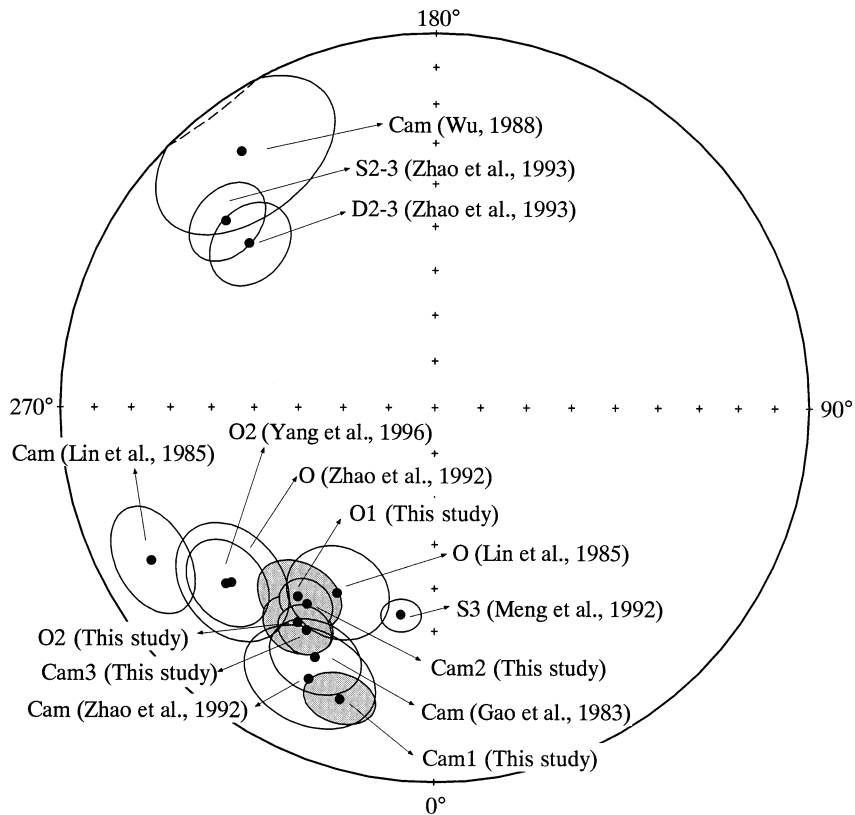


Fig. 13. Equal-area projection of the available early Paleozoic paleomagnetic poles with 95% confidence limits for the NCB. The poles of Zhao et al. (1992) are plotted with reversed polarity. All plotted onto lower hemisphere. *Cam*, *O*, *S*, and *D* represent Cambrian, Ordovician, Silurian, and Devonian, respectively, with 1 = Early, 2 = Middle, 3 = Late.

Table 8
The early Paleozoic paleomagnetic results from the NCB

Age	P _{long.} (°E)	P _{lat.} (°N)	A ₉₅ (°)	Dec. (°)	Inc. (°)	Paleolat. (°)	References
Middle Ordovician	327.7	31.5	7.0	327.8	-27.1	-14.4	This study
Early Ordovician	324.3	37.4	8.5	333.3	-20.4	-10.6	This study
Late Cambrian	329.6	31.7	5.4	326.5	-25.4	-13.4	This study
Middle Cambrian	326.7	37.0	5.5	331.4	-19.4	-10.0	This study
Early Cambrian	341.9	18.5	6.5	309.1	-31.8	-17.2	This study
Devonian	228.7	34.2	8.8	46.8	1.1	0.5	Zhao et al., 1993
Silurian	228.4	26.2	8.2	52.7	-9.6	-4.8	Zhao et al., 1993
Ordovician	130.9°E	28.8°S	12.3	160.7	40.0	22.8	Zhao et al., 1992
Cambrian	155.2°E	21.2°S	12.4	136.0	34.8	19.2	Zhao et al., 1992
Middle Ordovician	332.5	43.2	10.6	330.8	-4.8	-2.4	Lin et al., 1985
Cambrian	298.6	15.0	9.9	349.9	-58.1	-38.8	Lin et al., 1985
Middle Ordovician	310.4	27.9	9.2	340.8	-41.4	-23.8	Yang et al., 1996
Cambrian	334.5	26.8	8.9	320.1	-28.3	-15.0	Gao et al., 1983

Abbreviations: Paleolat., Dec. and Inc. = paleolatitude, declination and inclination, resp., of paleomagnetic directions calculated from the paleomagnetic poles (longitude/latitude) at reference site: Hancheng, Shaanxi Province (110.5°E/35.6°N). The rest same as Table 2.

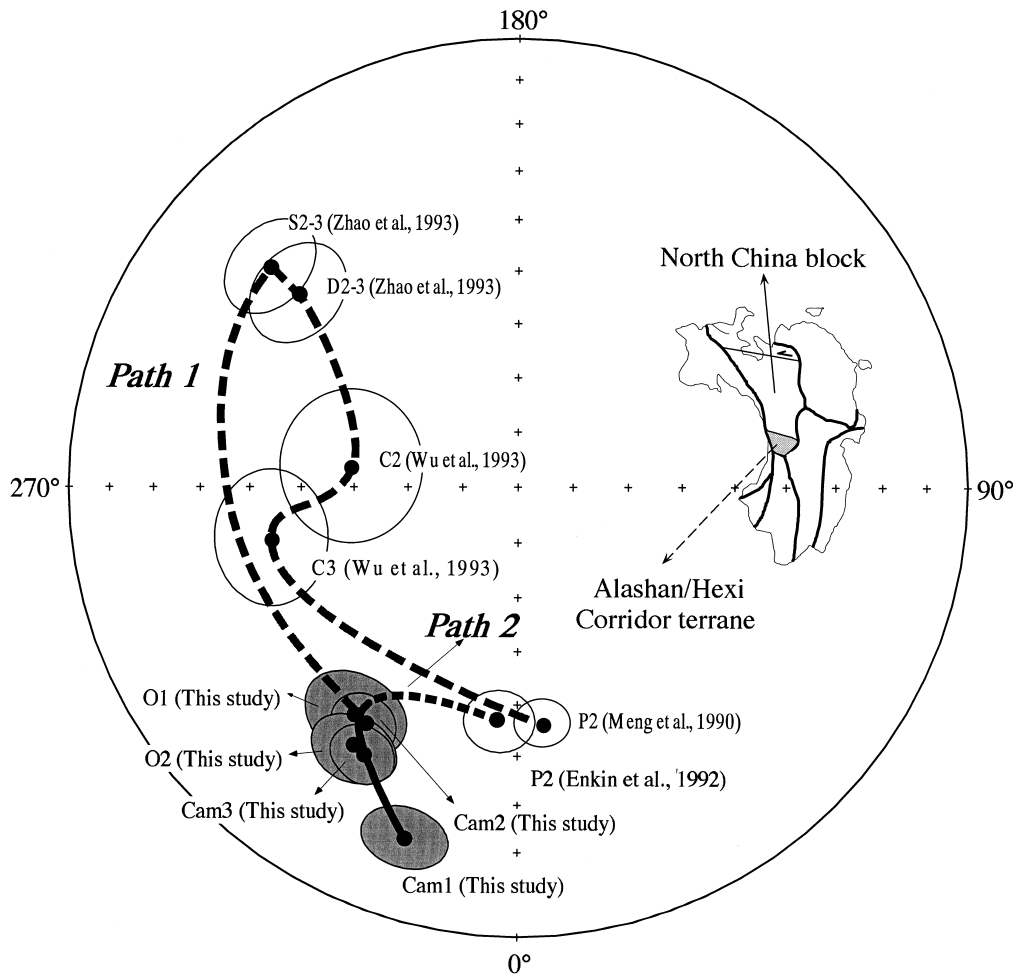
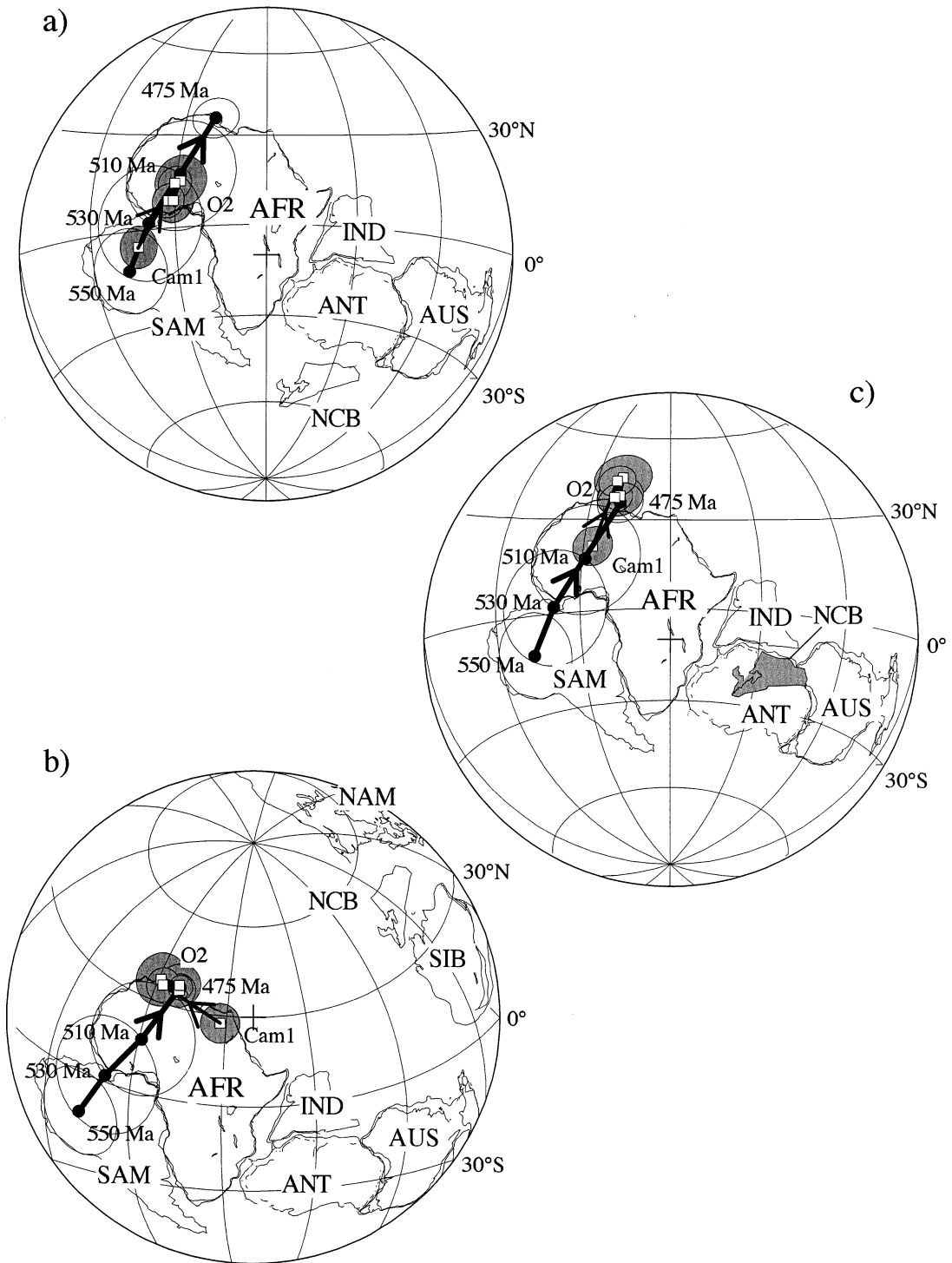


Fig. 14. Equal-area projection of the established early Paleozoic APWP for the NCB (solid line) and two possible APWP paths for the post-Middle Ordovician period. Path 1 suggests a Siluro–Devonian loop (shaded dashed line) if the Alashan/Hexi Corridor terrane is considered as a part of the stable NCB (see details in text). We welded the APWP for a period between the Cambrian and Ordovician with the Permian pole (Enkin et al., 1992) by dashed line in the figure (path 2); however, the post-Middle Ordovician movement of the NCB cannot be discussed in detail until more reliable Silurian and Devonian paleopoles for the NCB have been obtained. The rest same as Fig. 13.

a similar position to the Ordovician pole reported by Zhao et al. (1992). A Middle Ordovician pole (332.5°E , 43.2°N , $A_{95} = 10.6^{\circ}$) reported by Lin et al. (1985) clusters between our Early and Middle Ordovician poles and the Permian one for the NCB (Enkin et al., 1992). This Middle Ordovician pole might have been subjected to contamination by late Paleozoic overprint and was rejected by the original authors (Lin and Fuller, 1990).

Meng and Coe (1992) report a Late Silurian paleopole (Fig. 13; Table 8) from the purplish-red

sandstones and mudstones of the Hanxia Formation in the west of Hexi Corridor, Gansu Province (see Fig. 1 for the locality of the Alashan/Hexi Corridor). This pole is located close to the Permian one (Fig. 13), while it is claimed to pre-date the Caledonian folding at the end of the Silurian according to the positive fold test. No significant vertical rotation is then inferred for the NCB during that long period on the basis of little deviation between this Late Silurian pole and the Permian one for the NCB (Meng and Coe, 1992). At the same time, Zhao et al. (1993)



report two new Siluro–Devonian paleopoles from the redbeds, gray sandstones, one site in andesites, and a few limestones from widely distributed localities in the Alashan/Hexi Corridor terrane (Fig. 13; Table 8). A Siluro–Devonian loop could be postulated if we link our early Paleozoic poles to the Siluro–Devonian poles (Zhao et al., 1993) and the late Paleozoic poles from the NCB (Fig. 14, path 1), which could be inferred to be true polar wander (TPW) during this period (Van der Voo, 1994). However, this link is hampered by the following:

The different Silurian poles reported from the Alashan/Hexi Corridor terrane (Meng and Coe, 1992; Zhao et al., 1993) arouse suspicion about their reliability. Firstly, regional rotation with respect to the NCB is indicative of a suspect terrane for the Alashan/Hexi Corridor area. The Silurian, Devonian, Carboniferous and Permian paleopoles from the Alashan/Hexi Corridor terrane (Meng et al., 1990; Zhao et al., 1993; Wu et al., 1993) show about 90° of eastward polar wandering (Fig. 14). Secondly, the local rotation and tectonic deformation may not be excluded because complicated strike-slip faults cross the study areas. As demonstrated by Wu et al. (1993), internal displacement and deformation in the Alashan/Hexi Corridor terrane probably existed before the end of the Triassic. Finally, the late Paleozoic remagnetization may not have been completely removed because there is close correspondence between the Late Silurian pole (Meng and Coe, 1992) and the Permian one (Meng et al., 1990). The validity of the Siluro–Devonian pole position for the NCB is now open to question.

We therefore refrain from using them for construction of the early Paleozoic APWP for the NCB in this study.

5.3. Tectonic implications

Comparing our data with the previous Cambro–Ordovician paleopoles, we establish a new APWP for the early Paleozoic period of the NCB relying upon our early Paleozoic poles (Fig. 14). The NCB is firstly inferred to be located around 15° in the Southern Hemisphere during Cambro–Ordovician time (Table 8). Westward polar wandering by about 20° is secondly expected for the NCB during the Early Cambrian through middle Ordovician, which is much smaller than the nearly 70 to 90° polar wandering obtained from the Gondwana supercontinent (Meert and Van der Voo, 1997; Kirschvink et al., 1997). This implies that the NCB may not have been a part of Gondwanaland after the Early Cambrian.

The relationship between the NCB and Gondwana has been a matter of debate for a long time, and is partly due to the lack of longitudinal constraints in paleomagnetic study. The Cambrian TPW hypothesis during this period infers the uniform motion of the mantle relative to the spin axis, which may potentially be used to constrain the reconstruction of Gondwana relative to the NCB and the others. We note that our Cambro–Ordovician poles for the NCB correlate with those of Gondwana (Meert and Van der Voo, 1997), with the NCB sited adjacent to eastern Antarctica (Fig. 15a). This configuration is similar to that of Piper and Zhang (1997) deduced from a Neoproterozoic paleomagnetic study of glacial rocks for the NCB, and is also in accordance with recent paleontologic and paleogeographic evidence (Burrett et al., 1990). Nie (1991) also infers the low latitude for the NCB based on the paleobiogeographic and paleoclimatic results.

Our Cambro–Ordovician poles suggest that sig-

Fig. 15. Schematic maps showing reconstructions of the NCB with its adjacent regions of the world in (a) Early Cambrian, and (b and c) Middle Ordovician time in African coordinates. Relative longitudes of the blocks are unconstrained. The early Paleozoic APWP for Gondwanaland (solid circles) is drawn according to Meert and Van der Voo (1997) and Grunow (1995). The early Paleozoic APWP for the NCB (open squares) is drawn on the basis of our results with shaded 95% confidence limit. All the poles are plotted with paleo-south poles. Abbreviations are: *AFR* = Africa; *ANT* = Antarctica; *AUS* = Australia; *IND* = India; *NAM* = North America; *NCB* = North China block; *SAM* = South America; *SIB* = Siberia. Other abbreviations same as Fig. 13. North America and Siberia are positioned in (b) according to their middle Ordovician poles of Van der Voo (1993), while the NCB is sited close to North America and Siberia in the middle Ordovician, on the basis of the similarities of the Ordovician benthic trilobite assemblages in the NCB with those of Siberia and North America. Gondwanaland (Africa, Antarctica, Australia, India and South America) is shown according to rotation poles: Australia to Antarctica (Royer and Sandwell, 1989): 38.9°E, 2°S, $\Delta = -31.5^\circ$; Antarctica to Africa (Norton and Sclater, 1979): 327.3°E, 2.4°S, $\Delta = 55.4^\circ$; South America to Africa (Scotese and McKerrow, 1990): 327.8°E, 45.5°N, $\Delta = 58.2^\circ$; India to Africa: 221.4°E, 27.6°S, $\Delta = 61.2^\circ$. See text for further discussion.

nificant polar wandering occurred from east to west during the Early and Middle Cambrian. This motion reflects the tectonic motion of the NCB in that period: the NCB was subjected to counterclockwise rotation of $22.3 \pm 7.0^\circ$ accompanied by northward translation of $7.2 \pm 6.8^\circ$. A similar northerly latitude drift is also observed for Siberia and Baltica at approximately the same time (Smethurst et al., 1998; Torsvik et al., 1991), which is in contrast to that of Gondwanaland with a large counterclockwise rotation and a small amount of southward displacement. This implies that the latest Precambrian supercontinent (Pannotia; Powell, 1995) that consisted of Laurentia juxtaposed against a united Gondwana was geologically fleeting. As suggested by Dalziel (1992), the rifting of Laurentia culminated in continent–continent separation during the 550–530 Ma interval. Laurentia, Siberia and the NCB may have separated together from Pannotia before the middle Ordovician (Fig. 15b). We also note that the NCB is superimposed over Antarctica in the middle Ordovician paleogeographic reconstruction (Fig. 15c), given that the Cambro–Ordovician poles of the NCB correlate with those of Gondwana (Grunow, 1995; Meert and Van der Voo, 1997). This implies that the NCB may not have been a part of Gondwanaland during that period. The NCB is therefore inferred to be located close to Siberia and North America in the Middle Ordovician (Fig. 15b), as also suggested by the similarity between the Ordovician benthic trilobite assemblages in the NCB and those of Siberia and North America (Cocks and Fortey, 1990).

6. Conclusions

Characteristic remanent magnetizations were isolated from 281 samples of Cambrian and Ordovician sediments from the margin of the Ordos Basin, the western part of the NCB. They pass the fold and reversal tests, and are believed to be of primary origin.

An early Paleozoic APWP was established for the NCB based upon five early Paleozoic paleopoles. A single polarity of paleomagnetic directions from the Middle Ordovician Jinghe and Pingliang formations, and the late–Early Ordovician Lower Majiagou Formation of Shaanxi and Ningxia of North China

is recognized as of reversed polarity within a long interval of reversed polarity in the Early and Middle Ordovician. The early Paleozoic paleo-north poles for the NCB were all located in the present Atlantic Ocean. These pole positions imply that the NCB was situated in the Southern Hemisphere around 15°S during the Cambro–Ordovician. The NCB was probably flanked to East Gondwana in the Early Cambrian, which is also postulated for the Early Cambrian fauna between the NCB and Australia. The NCB may have separated from Gondwana in post–Early Cambrian, and may have sited close to Siberia and North America in the Middle Ordovician.

Acknowledgements

We wish to thank Prof. Q.Y. Wei, X.H. Ma for their helpful comments and enthusiastic encouragement through this study and thank Mr. S. Xu, J.P. Tong, W.W. Yan, S.X. Wang, Y.J. Liu, G.L. Hou and S.Y. Fan for their help in field exploring and laboratory experiments. We also wish to thank Drs. R. Van der Voo and J.D.A. Piper and an anonymous reviewer for their valuable comments and improvement of the manuscript. This work was supported by the National Nature Science Foundation of China (No. 49334050 and 49504052). The China–Japanese Government Culture Exchange Program supported B.C. Huang for his stay in Japan. Z.Y. Yang acknowledges the Inoue Foundation for Science of Japan and the JSPS for supporting his stay in Japan. Most of the figures were created using the PaleoMac software administered by Prof. Jean-Pascal Cogné.

References

- Algeo, T.J., 1996. Geomagnetic polarity bias patterns through the Phanerozoic. *J. Geophys. Res.* 101, 2785–2814.
- Audley-Charles, M.G., Ballantyne, P.D., Hall, R., 1988. Mesozoic–Cenozoic rift–drift sequence of Asian fragments from Gondwanaland. *Tectonophysics* 155, 317–330.
- Burrett, C., Long, L., Stait, B., 1990. Early–Middle Paleozoic biogeography of Asian terranes derived from Gondwana. *Geol. Soc. London Mem.* 12, 163–174.
- Cheng, Y.Q., 1994. An outline of regional geology of China (in Chinese). *Geol. Publ. House, Beijing*, 517 pp.
- Cocks, L.R.M., Fortey, R.A., 1990. Biogeography of Ordovician

- and Silurian faunas. *Geol. Soc. London Mem.* 12, 97–104.
- Dalziel, I.W.D., 1992. On the organization of American plates in the Neoproterozoic and the breakout of Laurentia. *GSA Today* 2 (11), 237–241.
- Dekkers, M.J., Mattei, J.-L., Fillion, G., Rochette, P., 1989. Grain-size dependence of the magnetic behavior of pyrrhotite during its low-temperature transition at 34 K. *Geophys. Res. Lett.* 16, 855–858.
- Enkin, R.J., Yang, Z.Y., Chen, Y., Courtillot, V., 1992. Paleomagnetic constrains on the geodynamic history of the major blocks of China from the Permian to the present. *J. Geophys. Res.* 97, 13953–13989.
- Gallet, Y., Pavlov, V., 1996. Magnetostratigraphy of the Moyero river section (northwestern Siberia): constraints on geomagnetic reversal frequency during the early Paleozoic. *Geophys. J. Int.* 125, 95–105.
- Gao, R.F., Huang, H.N., Zhu, Z.W., Liu, H.S., Fan, Y.Q., Qing, X.J., 1983. The study of paleomagnetism in northeastern Sino-Korean massif during Pre-late Paleozoic (in Chinese). Contribution to Project of Plate Tectonics of Northern China, 1, Geol. Publ. House, Beijing, pp. 264–274.
- Grunow, A.M., 1995. Implications for Gondwanaland of new Ordovician paleomagnetic data from igneous rocks in southern Victoria Land, East Antarctica. *J. Geophys. Res.* 100, 12598–12604.
- Gurarii, G.Z., Kropotkin, P.N., Pezner, M.A., Son, R.V., Trubik-ihin, M.V., 1966. Laboratory evaluation of the usefulness of North Korea sedimentary rocks for paleomagnetic studies, I. *Acad. Sci. USSR, Phys. Solid Earth* 11, 128–136.
- Halgedahl, S., Jarrard, R.D., 1995. Low-temperature behavior of single-domain through multidomain magnetite. *Earth Planet. Sci. Lett.* 130, 127–139.
- Huang, B.C., Wei, Q.Y., Zhu, R.X., 1995. Magnetic features of the Early Paleozoic rock units in the North China block (in Chinese with English abstract). *Acta Geophys. Sin.* 38, 796–805.
- Johnson, H.P., Patten, D.V., Tivey, M., Sager, W.W., 1995. Geomagnetic polarity reversal rate for the Phanerozoic. *Geophys. Res. Lett.* 22, 231–234.
- Kirschvink, J.L., 1980. The least-squares line and plane and the analysis of paleomagnetic data. *Geophys. J. R. Astron. Soc.* 62, 699–718.
- Kirschvink, J.L., Ripperdan, R.L., Evans, D.A., 1997. Evidence for a large-scale reorganization of Early Cambrian continental masses by inertial interchange True Polar Wander. *Science* 277, 541–545.
- Lin, J.L., Fuller, M., 1990. Paleomagnetism, North China and South China collision, and the Tan-Lu fault. *Philos. Trans. R. Soc. London A* 331, 589–598.
- Lin, J.L., Fuller, M., Zhang, W.Y., 1985. Preliminary Phanerozoic polar wander paths for the North and South China blocks. *Nature* 313, 444–449.
- Long, J., Burrett, C., 1989. Fish from the Upper Devonian of the Shan-Thai terrane indicate proximity to east Gondwana and south China terranes. *Geology* 17, 811–813.
- Lowrie, W., 1990. Identification of ferromagnetic minerals in a rock coercivity and unblocking temperature properties. *Geophys. Res. Lett.* 17, 159–162.
- McElhinny, M.W., 1964. Statistical significance of the fold test in paleomagnetism. *Geophys. J. R. Astron. Soc.* 8, 338–340.
- McFadden, P.L., 1990. A new fold test for paleomagnetic studies. *Geophys. J. Int.* 103, 163–169.
- McFadden, P.L., Jones, D.L., 1981. The fold test in Paleomagnetism. *Geophys. J. R. Astron. Soc.* 67, 53–58.
- McFadden, P.L., McElhinny, M.W., 1990. Classification of the reversals test in paleomagnetism. *Geophys. J. Int.* 103, 725–729.
- Meert, J.G., Van der Voo, R., 1997. The assembly of Gondwana 800–550 Ma. *J. Geodyn.* 23, 223–235.
- Meng, Z.F., Coe, R.S., 1992. The Late Silurian paleomagnetic results of the Hexi Corridor and its tectonic implication (in Chinese). *Sci. China, Ser. B22*, 531–536.
- Meng, Z.F., Huang, H.F., Chen, Y.Z., Coe, R.S., 1990. The Late Permian pole of the western Jiuquan basin (NW China) and its tectonic implication. *Acta Sedimentol. Sin.* 8, 58–65.
- Moskowitz, B.M., Jackson, M., Kissel, C., 1998. Low-temperature magnetic behavior of titanomagnetites. *Earth Planet. Sci. Lett.* 157, 141–149.
- Nie, S.Y., 1991. Paleoclimatic and paleomagnetic constraints on the Paleozoic reconstructions of south China, north China and Tarim. *Tectonophysics* 196, 279–308.
- Ningxia Bureau of Geology and Mineral Resources (NBGM), 1990. Regional geology of Ningxia Hui autonomous region (in Chinese with English abstract). Geol. Publ. House, Beijing, 552 pp.
- Norton, I.O., Sclater, J.G., 1979. A model for the evolution of the Indian Ocean and the breakup of Gondwanaland. *J. Geophys. Res.* 84, 6803–6830.
- Pavlov, V., Gallet, Y., 1998. Upper Cambrian to Middle Ordovician magnetostratigraphy from the Kulumbé river section (northwestern Siberia). *Phys. Earth Planet. Inter.* 108 (1), 51–61.
- Piper, J.D.A., Zhang, Q.R., 1997. Palaeomagnetism of Neoproterozoic glacial rocks of the Huabei Shield: the North China Block in Gondwana. *Tectonophysics* 283, 145–171.
- Powell, C.McA., 1995. Are Neoproterozoic glacial deposits preserved on the margins of Laurentia related to the fragmentation of two supercontinent? *Comment. Geology* 23, 1053–1054.
- Rochette, P., Fillion, G., 1989. Field and temperature behavior of remanence in synthetic goethite: paleomagnetic implication. *Geophys. Res. Lett.* 16, 851–854.
- Rochette, P., Fillion, G., Mattei, J.-L., Dekkers, M.J., 1990. Magnetic transition at 30–34 Kelvin in pyrrhotite: insight into a widespread occurrence of this mineral in rocks. *Earth Planet. Sci. Lett.* 98, 319–328.
- Royer, J.Y., Sandwell, D.S., 1989. Evolution of the Eastern Indian Ocean since the Late Cretaceous: constraints from Geosat altimetry. *J. Geophys. Res.* 94, 13755–13782.
- Scotese, C.R., McKerrow, W.S., 1990. Revised world maps and introduction. *Geol. Soc. London Mem.* 12, 1–21.
- Shaanxi Bureau of Geology and Mineral Resources (SABGM), 1989. Regional geology of Shaanxi Province (in Chinese with English abstract). Geol. Publ. House, Beijing, 689 pp.

- Shanxi Bureau of Geology and Mineral Resources (SBGMR), 1989, Regional geology Shanxi Province (in Chinese with English abstract). Geol. Publ. House, Beijing, 780 pp.
- Smethurst, M.A., Khramov, A.N., Torsvik, T.H., 1998. The Neoproterozoic and Palaeozoic palaeomagnetic data for the Siberia Platform: from Rodinia to Pangea. *Earth Sci. Rev.* 43, 1–24.
- Torsvik, T.H., Ryan, P.D., Trench, A., Harper, D.A.T., 1991. Cambrian–Ordovician paleogeography of Baltica. *Geology* 19, 7–10.
- Van der Voo, R., 1993. Paleomagnetism of the Atlantic, Tethys, and Iapetus Oceans. Cambridge Univ. Press, New York, 441 pp.
- Van der Voo, R., 1994. True polar wander during the middle Paleozoic? *Earth Planet. Sci. Lett.* 122, 239–243.
- Wu, H.N., 1988. Apparent polar wander paths and paleolatitude distributions for the north and south China blocks: the geotectonic evolution of Qinling belt (in Chinese with English abstract). Ph.D. Thesis, Academia Sin., Beijing, 175 pp.
- Wu, H.N., Zhou, L.F., Zhao, Z.Y., Yang, Z.Y., Chen, Y., 1993. Tectonic implications of the paleomagnetic results of the later Paleozoic and Mesozoic rocks from the Alashan area of the western North China block. *Sci. Geol. Sin.* 2, 19–46.
- Yang, Z.Y., Cheng, Y.Q., Wang, H.Z., 1986. The Geology of China. Clarendon Press, Oxford, 303 pp.
- Yang, Z.Y., Sun, Z.M., Ma, X.H., Huang, B.C., Dong, J.M., Zhou, Y.X., Zhu, H., 1996. Preliminary paleomagnetic results from the Lower Paleozoic of North China (Henan Province) and its implications (in Chinese). *Chin. Sci. Bull.* 42, 401–405.
- Zhou, Y.X., Zhu, H., 1996. Preliminary paleomagnetic results from the Lower Paleozoic of North China (Henan Province) and its implications (in Chinese). *Chin. Sci. Bull.* 42, 401–405.
- Zhao, X.X., Coe, R.S., Liu, C., Zhou, Y.X., 1992. New Cambrian and Ordovician paleomagnetic poles for the North China block and their paleo-geographic implications. *J. Geophys. Res.* 97, 1767–1788.
- Zhao, X.X., Coe, R.S., Wu, H.N., Zhao, Z.Y., 1993. Silurian and Devonian paleomagnetic poles from North China and implications for Gondwana. *Earth Planet. Sci. Lett.* 117, 497–506.
- Zhao, X.X., Coe, R.S., Zhou, Y.X., Hu, S.Y., Wu, H.R., Kuang, G.D., Dong, Z.G., Wang, J., 1994. Tertiary paleomagnetism of North and South China and a reappraisal of late Mesozoic paleomagnetic data from Eurasia: implications for the Cenozoic tectonic history of Asia. *Tectonophysics* 235, 181–203.
- Zhao, X.X., Coe, R.S., Gilder, S.A., Frost, G.M., 1996. Paleomagnetic constrains on the paleogeography of China: implications for Gondwanaland, Australia. *J. Earth Sci.* 43, 643–672.
- Zijderveld, J.D.A., 1967. A.C. demagnetization of rocks: analysis of results. In: Collinson, D.W., Creer, K.M., Runcorn, S.K. (Eds.), *Methods on Paleomagnetism*. Elsevier, New York, pp. 245–286.